Materials Today • Volume xxx, Number xx • xxxx 2022 RESEARCH

ELSEVIER

Advances in triboelectric nanogenerator powered electrowetting-on-dielectric devices: Mechanism, structures, and applications

RESEARCH: Review

Jie Tan [1,2], Shulan Sun [3], Dongyue Jiang [1,*], Minyi Xu [4,*], Xiangyu Chen [2,*], Yongchen Song [1], Zhong Lin Wang [2,5,*]

[1] Key Laboratory of Ocean Energy Utilization and Energy Conservation of Ministry of Education, Dalian University of Technology, 116024, China
[2] Beijing Institute of Nanoenergy and Nanosystems, Chinese Academy of Sciences, Beijing, 100083, China
[3] Cancer Hospital of Dalian University of Technology (Liaoning Cancer Hospital & Institute), Shenyang 110801, China
[4] Dalian Key Laboratory of Marine Micro/Nano Energy and Self-powered Systems, Marine Engineering College, Dalian Maritime University, Liaoning Province, 116026, China
[5] School of Materials Science and Engineering, Georgia Institute of Technology, Atlanta, GA, USA

Electrowetting-on-dielectric (EWOD) phenomenon is widely employed for liquid actuation at the micro scale. Due to its simple structure, low cost, low power consumption and fast response speed, diverse applications are developed and commercialized based on EWOD, such as digital microfluidics, tunable lenses, electronic displays, small-scale propellers *etc*. However, the liquid actuation with EWOD requires a high-voltage but low-current power source. The accessory equipment (*e.g.,* waveform generator and amplifier) not only attenuates the benefits originated from microscale liquid actuation, but also limits its portability, wearability, and environmental friendliness of the EWOD inspired applications. Triboelectric nanogenerator (TENG) is a promising technology to convert arbitrary mechanical energy to electricity based on triboelectrification and electrostatic induction. The output electric signal shows a high-voltage but low-current property which well matches the demands in EWOD devices. This paper reviews the technical advances in the TENG powered EWOD devices developed in recent years. The mechanisms, structures, and performance of each application are reviewed. The challenges and future perspectives are put forward. The review and discussion in this study open up opportunities for the development of TENG and EWOD based self-powered liquid actuators.

Introduction

Electrowetting refers to the phenomenon of the modulation of wetting property (*e.g.,* contact angle) of aqueous phase on an electrode surface by the applied electric potentials (terminals of voltage source are connected with aqueous solution and electrode separately). The electrowetting of mercury on charged surfaces was first observed and explained by Gabriel Lippmann in 1875 [1] Due to the direct contact between mercury and electrode, electrolysis easily occurs and induces instability in the electrowetting phenomenon. In 1969, Dahms [2] introduced the electrowetting-on-dielectric (EWOD) configuration by using an insulating layer to separate the aqueous phase from the electrode. The dielectric layer effectively prevents the occurrence of electrolysis and enlarges the range of applied electric potential from several volts to hundreds of volts. In 1993, Bruno Berge [3] combined Young's wetting theory with Lippmann's theory and derived the relationship between the contact angle modulation with the applied electric potential. With an extra hydrophobic coating on top of the dielectric layer in the modern EWOD design, a large range of reversible contact angle modulation

* Corresponding authors.
E-mail addresses: Jiang, D. (jiangdy@dlut.edu.cn), Xu, M. (xuminyi@dlmu.edu.cn), Chen, X. (chenxiangyu@binn.cas.cn), Wang, Z.L. (zlwang@binn.cas.cn).

1369-7021/ https://doi.org/10.1016/j.mattod.2022.07.009

Please cite this article in press as: J. Tan et al., Materials Today, (2022), https://doi.org/10.1016/j.mattod.2022.07.009

could be achieved between 110° and 65° for an aqueous solution. Such a large and robust contact angle modulation inspires the development of diverse applications in the fields of lab-on-a-chip [4], point-of-care (POC) [5], biomedical [6,7], chemical [8], optical [9], robotics [10,11], motors [12] *etc*. Among these applications, digital microfluidics (DMF) [13] and optical devices (tunable lenses [14], electronic display [15]) have been rapidly developed and commercialized in recent years.

Inspired by the EWOD phenomenon, the digital microfluidics (DMF) [16] platform was firstly developed for chemical and biological applications in the forms of lab-on-a-chip synthesis and diagnostics [17]. By activating the patterned electrodes on the DMF platform, the contact angle of the microdroplet on top of the DMF platform could be modulated asymmetrically. The asymmetric contact angle induces the Laplace pressure difference inside the microdroplet to achieve actuation [18]. Based on the mechanism of single droplet actuation, functions including droplet transportation, splitting, dispense, two droplets merging, and parallel droplets actuations were developed. These basic functions were further upgraded as low-voltage droplet actuation [19–21], opto-electrowetting (OEW) droplet actuation [22–24], anti-biofouling actuation [25] and so on. Compared to the flow-through type microfluidics, the DMF platform offers advantages of even smaller sample volume, better organic solvent adaptability (without PDMS), automation and multi-step reaction feasibility. Nowadays, the DMF platform has been widely employed and commercialized for single cell analysis [26], immunoassay [27], DNA amplification [28], enzymatic test [29], radiochemistry synthesis [30] and so on. Except for the applications in the DMF platform, the EWOD phenomenon also inspired the rapid development of tunable optics and reflective electronic displays. Liquid lenses with tunable focal lengths could be formed by two immiscible liquids with different refractive indices [31]. By tuning the contact angle of the aqueous phase electronically, the shape of the interface between the two immiscible liquids could be changed dynamically to form a varifocal lens. As compared to the conventional solid lenses, the liquid lenses provide the benefits of focal length tunability, less costly and wear-proof. Similar to the liquid lenses, the EWOD based electronic display [9] has proven its advantages in an outdoor display, fast response speed and low power consumption.

The EWOD has been proven to be a powerful tool for liquid handling on capillary scale and inspired diverse applications. However, due to the fact that EWOD requires an electrostatic force applied to the vicinity of the liquid–solid-gas three phase contact lines to achieve actuation [14]. The employed power source for creating such an electrostatic field [32] to an EWOD device is different from the resistor-type loads, a high voltage but low current source is typically required as accessory equipment. The accessory equipment includes a waveform generator, amplifier and control circuit. The equipment significantly attenuated the benefits from the microscale liquid handling device, which is promising for portable, distributed, and point-of-care applications. For example, wristband DMF platform [33] has been proven to be applicable for real-time healthcare monitoring towards point-of-care (POC) application. However, the accessory power source limits the practical application since the accessory equipment is difficult to be wearable. Furthermore, the employment of chemical batteries and electricity from the grid also increases the burden on pollution and environmental protection. In order to take full advantage of EWOD inspired DMF platform, tunable lenses as well as other emerging applications, a self-powered, light-weight and clean power source is highly desired.

In 2012, Wang et al. proposed the triboelectric nanogenerator (TENG) as an energy harvesting device to convert the random and unordered mechanical energy into electricity [34]. TENG has attracted extensive attention due to its high conversion efficiency [35,36], wide availability of constituent material [35], large tolerance to mechanical stimuli and easy fabrication [18,37]. The mechanism of TENG is based on triboelectrification and electrostatic induction [38,39]. There are four major working modes of TENG devices, including contact-separation mode [40], single-electrode mode [41], lateral sliding mode [42], and free-standing triboelectric layer mode [43]. Different from the electromagnetic generators which require high- speed rotation of the windings to encircle the magnetic flux to induce Lorenz force for electrons movement [44], TENG could harvest types of mechanical energy, including sliding, vibrating [45], swimming [46], elastic deformation *etc*., which enables the energy harvesting from a broad source of mechanical energy such as wind energy [47–49], ocean wave energy [50–52] to be converted into electricity. Especially in low-frequency conditions, the TENG shows better output performance as compared to the EMG of the same size [53]. This superior feature of TENG allows for harvesting low-frequency biomechanical energy (*e.g*. body movement [54,55], breathing [56], and heart beating) [57]. These superior properties of TENG have boosted the rapid development of self-powered sensors [58–65], which incorporate the features of portability [66,67], self-powered, implantable [68–71], light-weight [72–74] and wearability [75–81].

The studies on TENG driven self-powered sensors had been well summarized in several review articles [82–87]. As compared to the TENG powered sensors, due to impedance matching, the TENG powered EWOD device shows great potential towards self-powered actuators. As shown in Fig. 1, diverse TENG powered EWOD devices have been reported in recent years with TENG harvesting mechanical energy from wide sources (*e.g*., wind, wave, human motion), but a comprehensive review is this topic is lacked. In this review, the recent advances in TENG powered EWOD devices (self-powered DMF, tunable lenses, and emerging technologies) are comprehensively reviewed. The working principles of TENG, EWOD and TENG powered EWOD devices are discussed in Section “Mechanisms, structures and materials of TENG powered EWOD”. The research status on TENG driven EWOD devices are reviewed in Section “EWOD devices powered by TENG” (including TENG driven DMF in “Digital microfluidics (DMF) driven by TENG”, TENG driven optical device in “EWOD based optical devices driven by TENG” and TENG driven emerging technologies in “EWOD based emerging technologies driven by TENG”). The challenges and future perspectives are discussed in Section “Summary and perspectives”.

Please cite this article in press as: J. Tan et al., Materials Today, (2022), https://doi.org/10.1016/j.mattod.2022.07.009

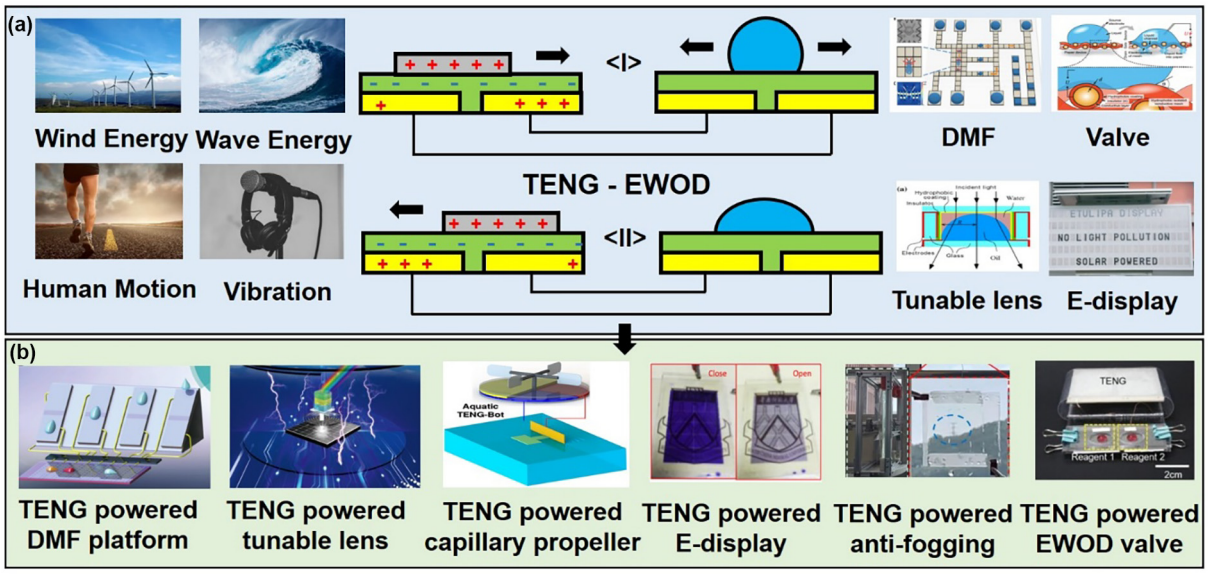

FIGURE 1

Recent demonstrations of TENG powered EWOD devices. In which TENG could be employed for harvesting mechanical energy from wind, wave, biomechanical *etc.*, while EWOD could be employed for DMF platform, tunable lenses, electronic display as well as emerging technologies (capillary propeller, anti-fogging etc.). The combination of TENG and EWOD boosts the rapid development of series self-powered liquid actuators. Reproduced with permission [88]. Copyright 2020, The American Association for the Advancement of Science. Reproduced with permission [89]. Copyright 2017, Wiley-VCH. Reproduced with permission [90]. Copyright 2004, American Institute of Physics. Reproduced with permission [91]. Copyright 2020, Royal Society of Chemistry. Reproduced with permission [92]. Copyright 2018, Royal Society of Chemistry. Reproduced with permission [93]. Copyright 2021, Elsevier. Reproduced with permission [94]. Copyright 2020, American Chemical Society. Reproduced with permission [95]. Copyright 2019, Elsevier. Reproduced with permission [96]. Copyright 2022, Elsevier. Reproduced with permission [97]. Copyright 2019, Wiley-VCH.

Mechanisms, structures and materials of TENG powered EWOD

Mechanism of EWOD

Since the first observation of electrowetting (EW) phenomenon in 1875 by Lippmann [1], the relationship between the differential of interfacial tension, surface charge density and electric potential is given as $d\sigma_{SL}^{eff} = -\rho_{SL}dU$. When integrating the relationship of Young's equation $(\sigma_{SV} = \sigma_{SL} - \sigma_{LV}\cos(\theta))$ which describes the relationship between interfacial tension and contact angle with Lippmann's equation, the Young-Lippmann equation describing the EW phenomenon could be derived as:$\cos(\theta) = (\sigma_S - \sigma_{SL}^0 + CV^2/2)/\sigma_L$. This formula describes the EW phenomenon where the capacitance is formed by the electrical double layer (EDL) between liquid and electrode. The EDL layer with a thickness of Debye length (~tens of nanometers) yield a large specific capacitance, leading to a large contact angle variation when a small voltage is applied. However, electrolysis easily occurs in this system and few practical applications were demonstrated based on EW. When Dahms incorporates an insulating layer into the EW system, the full description of EWOD phenomenon was described by Bruno Berge as shown in Eq. (1) [98]. In which V is the electric potential between the liquid and the dielectric, θ is the contact angle of the liquid on the solid surface, θ_0 is the initial contact angle (CA), ε_0 is the vacuum dielectric constant, ε_r is the relative permittivity of the insulating layer, σ_{LV} is the interfacial tension between liquid and gas, and d is the thickness of the dielectric layer.

$$\cos\theta = \cos\theta_0 + \frac{\varepsilon_0\varepsilon_r}{2\sigma_{LV}d}V^2 \quad (1)$$

The above equation could be intuitively illustrated in Fig. 2 which shows a top-electrode EWOD device. When zero electric potential is applied, the droplet remains a spherical shape on a hydrophobic surface (Fig. 2a). When a non-zero electric potential is applied, the contact angle of the droplet reduces following a trend of the cosine function (Fig. 2b). With this mechanism, the microfluidic phenomenon such as droplet actuation, two-phase flow modulation, and capillary wave generation could be induced for the applications of DMF, tunable lenses, electronic display and emerging technologies (capillary wave propeller, anti-fogging glass).

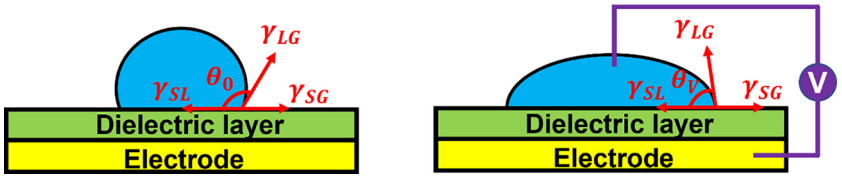

FIGURE 2

Working mechanism of EWOD.

Please cite this article in press as: J. Tan et al., Materials Today, (2022), https://doi.org/10.1016/j.mattod.2022.07.009

Mechanism of TENG

On the other side, the triboelectric effect shows the same device structure as the planar EWOD device. The difference is that by moving the solid or liquid above the patterned and dielectric coated electrodes, due to contact electrification and electrostatic induction, alternating-current (AC) electric current could be attained between the two electrodes. The TENG device could be employed for harvesting the mechanical energy from a broad range of sources, including wind energy, vibration, wave energy and even biomechanical energy. The driving force for the TENG is the Maxwell's displacement current, which is caused by a time variation of electric field plus a media polarization term. In the case of TENGs, triboelectric charges are produced on surfaces simply due to contact electrification between two different materials. To account for the contribution made by the contact electrification induced electrostatic charges in the Maxwell's equations, an additional term P_s, called mechano-driven produced polarization, is added in displacement vector D by Wang [39], that is.

$$D = \varepsilon_0 E + P + P_s \tag{2}$$

Here, the first term polarization vector P is due to the existence of an external electric field, and the added term P_s is mainly due to the existence of the surface charges that are independent of the presence of electric field and the relative movement of the media. Substituting Eq. (2) into Maxwell's equations, and define.

$$D' = \varepsilon_0 E + P \tag{3}$$

The reformulated Maxwell's equations are [99].

$$\nabla \cdot D' = \rho_f - \nabla \cdot P_s \tag{4.1}$$

$$\nabla \cdot B = 0 \tag{4.2}$$

$$\nabla \times E = -\frac{\partial B}{\partial t} \tag{4.3}$$

$$\nabla \times H = J + \frac{\partial P_s}{\partial t} + \frac{\partial D'}{\partial t} \tag{4.4}$$

In Eq. (4.4), $\frac{\partial D'}{\partial t}$represents the displacement current due to time variation electric field and the electric field induced medium polarization. The second term $\frac{\partial P_s}{\partial t}$ is the displacement current due to non-electric field but owing to external strain field. The first term is dominant at high frequency for wireless communication, while the second term is the low frequency or quasi-static term that is responsible for the energy generation. The term that contributes to the output current of TENG is related to the driving force of $\frac{\partial P_s}{\partial t}$, which is simply named as the Wang term in the displacement current. In general cases, the two terms are approximately decoupled and can be treated independently. However, if the external triggering frequency is rather high, so that the two terms $\frac{\partial D'}{\partial t}$ and $\frac{\partial P_s}{\partial t}$ can be effectively coupled, the interference between the two term can be significant, but such case may occur in MHz - GHz range. The Maxwell's equations for mechano-driven slow-moving media system are shown in Fig. 3.

The conventional Maxwell's equations are for media whose boundaries and volumes are fixed and at stationary. But for cases that involve moving media and time-dependent configuration, such as the case in TENG, the equations have to be expanded. Starting from the integral forms of the four physics laws, Wang has derived the expanded Maxwell's equations in differential form by assuming that the medium is moving as a rigid translation object with acceleration. If the relativistic effect is ignored, the Maxwell's equation for a mechano-driven slow-moving media system is given by [100].

$$\nabla \cdot D' = \rho_f - \nabla \cdot P_s \tag{5.1}$$

$$\nabla \cdot B = 0 \tag{5.2}$$

$$\nabla \times (E - v \times B) = -\frac{\partial}{\partial t} B \tag{5.3}$$

$$\nabla \times [H + v \times (D' + P_s)] = J_f + \rho_f v + \frac{\partial}{\partial t} Ps + \frac{\partial}{\partial t} D' \tag{5.4}$$

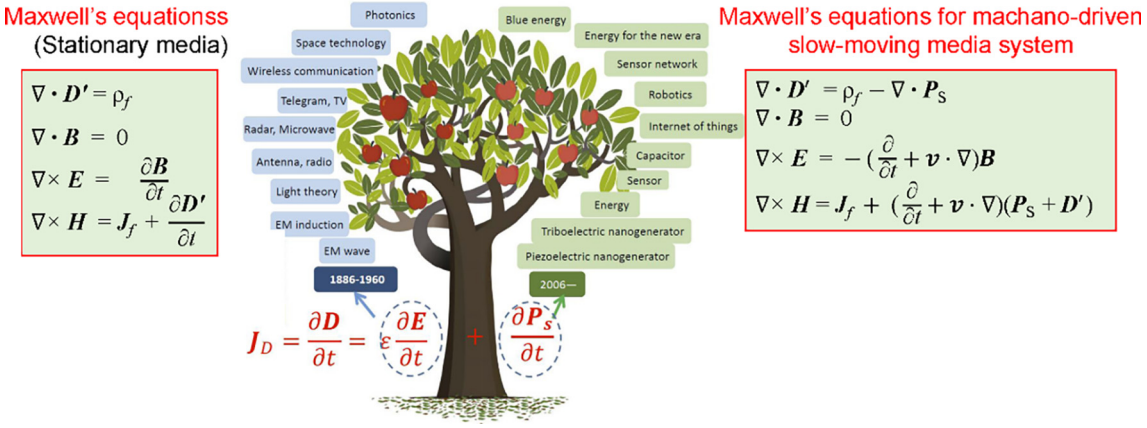

FIGURE 3

The conventional Maxwell's equations are for media whose boundaries and volumes are fixed and stationary. The Maxwell's equations for a mechano-driven slow-moving media system are further developed with including the polarization density term P_s in displacement vector. These equations apply to media that moves with an acceleration in non-inertia frame of references. Note the equations given at the right-hand side are identical to those given in Eqs. (5.1)–(5.4) if the media movement is rigid translation.

Please cite this article in press as: J. Tan et al., Materials Today, (2022), https://doi.org/10.1016/j.mattod.2022.07.009

It is important to note that the moving velocity is time dependent and the media is assumed to be rigid object. The only requirement is that the moving velocity is much less than the speed of light in vacuum with the ignorance of relativistic effect. These equations are most useful for describing the electromagnetic behavior of moving media with acceleration, and they are fundamentals for dealing with the coupling among mechano-el ectric–magnetic multi-fields and the interaction. The expanded equations are the most comprehensive governing equations including both electromagnetic interaction and power generation as well as their coupling for TENG.

Mechanism of TENG powered EWOD

It could be observed from Fig. 4a that the TENG and EWOD devices show the same structure but reverse processes: TENG harvests the mechanical energy to trigger the motion of the top solid or liquid for power generation, while the EWOD utilized the electricity to move the droplet. It is noteworthy that the analogy not only happens to freestanding mode TENG and planar EWOD devices, but also to the contact separation mode TENG and the top electrode mode EWOD devices. This reverse process could be analogous to the electromagnetic generator and electric motor. The term "reverse electrowetting (REWOD)" was first presented in 2011 to describe the energy harvesting device that employs a droplet sliding along a planar EWOD device [101,102].

The working mechanism of TENG powered EWOD device in diverse configurations could be found in Fig. 4b. The TENGs working in freestanding (FS) and contact separation (CS) modes were employed for triggering planar and top-electrode mode EWOD devices. As for the freestanding mode TENG, the sliding of the positively charged nylon film screens the positive charges to the left and right electrodes of the TENG. Since the TENG and planar EWOD devices share a same pair of electrodes, the biased charge distribution appears on the EWOD electrodes accordingly for contact angle modulation. In stage <i>, the nylon film stays in the middle of the two electrodes, thus the left and right electrodes hold the same amount of positive charges, a symmetric contact angle is found on the planar EWOD device. In stage <ii>, the nylon film moves the right electrode, revealing the left electrode with excess positive charges. Due to the unbalanced charge distribution on the left and right electrodes, the droplet on the EWOD devices shows a reduced left side contact angle. When the nylon film further moves back to the left electrode, a reverse process happens and the right-side contact angle of the droplet reduces. Similarly, as for the contact separation mode TENG, when the PTFE film leaves contact with the nylon film as shown in stage <ii>, the charges are screened to the electrode of the EWOD device, contributing to a reduced contact angle of the droplet. When the PTFE film contacts with the nylon film again as shown in stage <iv>, charge transfer happens and the contact angle reduces accordingly.

As shown in Fig. 4a, the contact electrification for TENG could be achieved either between solid and solid or between liquid and solid. The liquid–solid TENG configuration is exactly the same as the EWOD device. However, whether the two devices share a reverse physical process still require further exploration. As for the solid–liquid TENG, traditional view holds that the reason for the electrification of liquid–solid contact is ion transfer without considering the contribution of electron transfer. Lin et al. [103] confirmed the existence of electron transfer in the electrification process of liquid–solid contact from a microscopic perspective using Kelvin probe force microscopy and electron thermal excitation theory. A two-step model for solid–liquid triboelectrification is proposed [104] which shows the electron transfer is followed by ion transfer and the two processes are independent. Based on the studies of Zhang [105] and Zhan et al. [106], on the gradual saturation process of the contact charge between water droplets and polymers, it is proved that the electrification of liquid–solid contact is the result of the combined effect of electron transfer and ion transfer, which could be

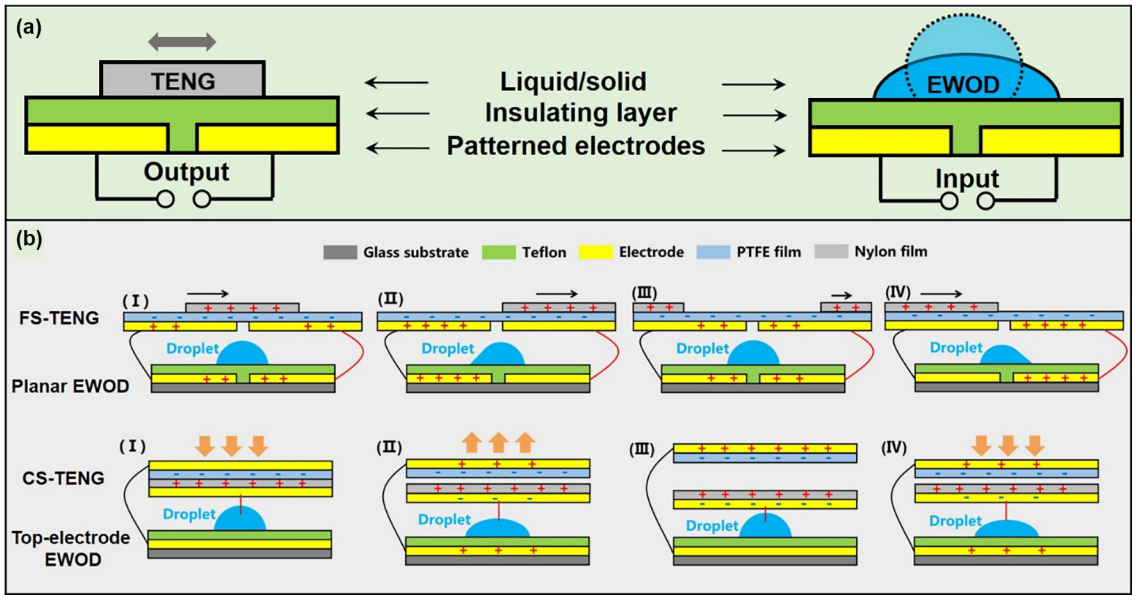

FIGURE 4

Device configuration and working mechanism of TENG powered EWOD device.

Please cite this article in press as: J. Tan et al., Materials Today, (2022), https://doi.org/10.1016/j.mattod.2022.07.009

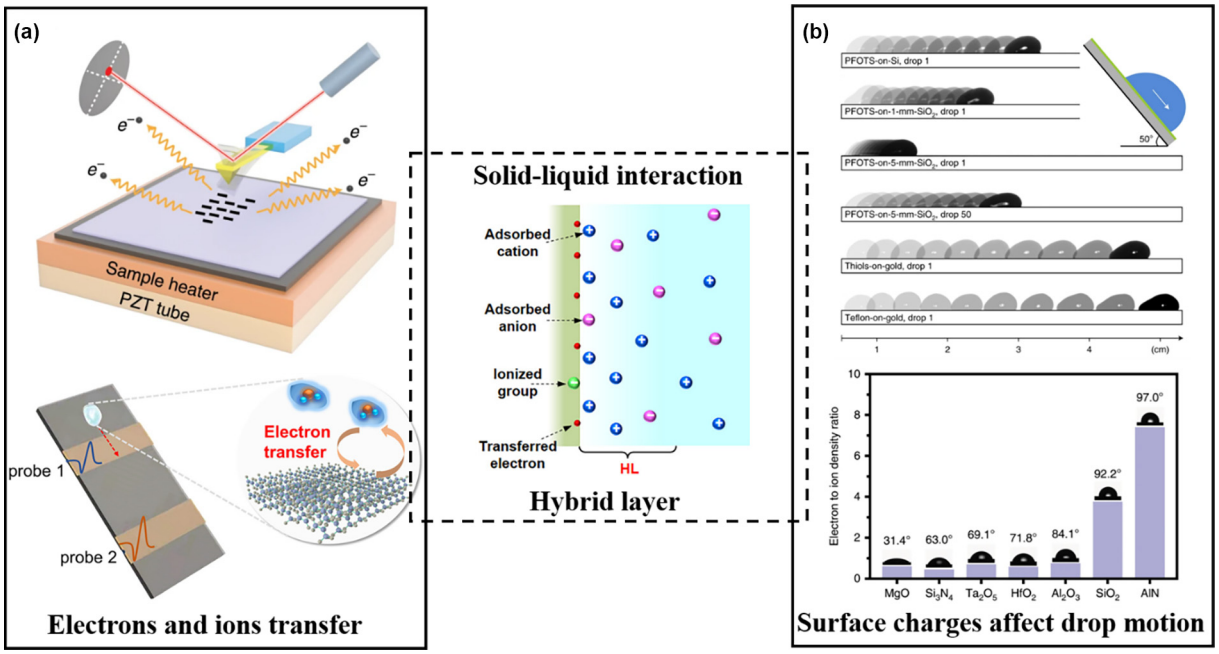

FIGURE 5

Solid-liquid interaction. Electrons and ions transfer in the solid–liquid TENG devices. The sliding motion and CA of a droplet are affected by the surface charges. Both the two processes are related to the solid–liquid interaction in the hybrid layer. Reproduced with permission [103]. Copyright 2020, Nature Publishing Group. Reproduced with permission [105]. Copyright 2021, American Chemical Society. Reproduced with permission [106]. Copyright 2020, American Chemical Society. Reproduced with permission [107]. Copyright 2022, Nature Publishing Group. Reproduced with permission [103]. Copyright 2020, Nature Publishing Group.

modelled by Wang's Hybrid layer as shown in Fig. 5. On the other hand, the effects of surface charges on the droplet dynamics on solid surfaces have been reported recently. The surface charges were demonstrated to influence the sliding motion [107,108] as well as the static CA [103] of the droplet as shown in Fig. 5. The static CA of water was reported to be related to the ratio of electron transfer to ion transfer. However, in EWOD devices, the dynamics of the droplet is dominated by the charge transfer induced CA modulation. The initial surface charges contribute less to the variation of CA modulation because the surface charges and ions in the electrolyte form an electric double layer (EDL) with a large enough specific capacitance due to the small thickness of Debye length (~tens of nanometers). The specific capacitance of the hydrophobic insulating layer is much smaller since this layer is typical with a thickness of hundreds of nanometers to tens of microns. In a serially connected capacitance model, the total capacitance is typically dominated by the small one (the hydrophobic insulating layer). However, when the EWOD device operates for repeated cycles and the surface charges accumulate to a certain extent, the EWOD device was reported with poor stability due to the electrostatic forces between the surface charges and the droplet to be actuated.

Inspired by the similar output and input signal characteristics (large voltage but small current) of TENG and EWOD devices, several researchers have proposed and studied the TENG powered EWOD devices for the applications towards self-powered DMF, tunable lenses, capillary propulsion *etc*. The mechanism of employing the motion of part of TENG to trigger the motion of another droplet (or object) on EWOD device is termed as "water powered remote transfer of kinetic energy" in some studies [109]. It is noteworthy that the droplet movement on the EWOD device could also induce transfer process of electrons and ions. However, the TENG device for driving the EWOD typically employs a large enough moving part compared to the droplet to be actuated for eliminating the negative effect induced by triboelectrification between the droplet and the EWOD device.

Structures and materials of TENG powered EWOD

Different modes of TENG can be applied to different working environments, and the selection and processing of triboelectric materials have a great impact on the output performance. Zou et al. [110] introduced a universal standard method to quantify the triboelectric series for a wide range of polymers, establishing quantitative triboelectrification as a fundamental materials property. In various applications of EWOD, a wider range of CA variations is often pursued. This is directly related to the physical parameters of the dielectric layer and the hydrophobic layer. EWOD applications typically require a large Young's angle (for maximum change in modulated CA) and low wetting hysteresis for more accurate modulation and modulation without a threshold hysteresis to overcome. Most commercial EWOD devices use oil as insulating fluid because it provides a very large Young's angle and low wetting hysteresis. On the other hand, the material selection and thickness of the dielectric layer are very critical to the operation of the EWOD devices. Regarding the selection and performance of materials in EWOD devices, Table 1 compares the material selection, peak voltage and application method for both TENG and EWOD [111].

Please cite this article in press as: J. Tan et al., Materials Today, (2022), https://doi.org/10.1016/j.mattod.2022.07.009

TABLE 1

Material selection and treatment for TENG powered EWOD devices.

TENG work model	Triboelectric materials	TENG Surface treatment	TENG output performance	EWOD materials	Application	Refs.
Lateral sliding	Kapton/FEP	ICP	~1.8 kV (Vpp) 1–10 Hz	FEP	DMF	[113]
Freestanding	Kapton/FEP	ICP	~3.5 kV (Vpp) 7.2μA	PTFE/FEP	DMF	[113]
Freestanding	Kapton/Al	–	~3.4 kV (Vpp) 8.5μA 0.5 Hz	PCAS	DMF	[114]
Water-TENG	Water/Teflon	–	30–50 V	Teflon	DMF	[92]
Contact-separation	Silk/PVA&MXene	Electrospinning	118.4 V 1–30 Hz	FEP/Teflon	DMF	[115]
Rotating freestanding	Nylon/PTFE	–	1.4–3.5 kV(Vpp)	PDMS/FEP	DMF	[116]
Contact-separation	Silicone/Al	DIW	124 V 1–10 Hz	Fluoropolymer	Display	[95]
Lateral sliding	Kapton/FEP	–	~3.5 kV (Vpp)	FEP	Liquid lens	[117]
Freestanding	Cu/FEP	–	~530 V(Vpp) 1.2 μA	Teflon	Liquid lens	[93]
Contact-separation	Al/PTFE	ICP	~380 V(Vpp) 8μA	Parylene-C	EWOD valve	[118]
Freestanding	Cu/FEP	–	~520 V(Vpp) ~ 5μA 2 Hz	Teflon	Capillary Propeller	[94]
Rotating freestanding	Nylon/FEP	–	~0.73–5.26 kV(Vpp) 20–100 Hz	Teflon	Anti-fogging	[96]
Rotating freestanding	Sponge/PTFE	Oxygen plasma	~200 V(Vpp) 1–11.4 Hz	SiO_2	Micromolding	[119]
Contact-separation	Al/FEP	–	~5 kV (Vpp)	SU-8/Teflon	Wearable sensor	[120]

EWOD devices powered by TENG

Due to the impedance matching between the TENG and EWOD devices, diverse TENG powered EWOD devices towards a self-powered liquid actuators have been developed in recent years [121]. This section reviews the achievements in this field in terms of TENG powered DMF platform, TENG powered optical devices (electronic display and tunable lenses), and TENG powered EWOD based emerging technologies.

Digital microfluidics (DMF) driven by TENG

Among the EWOD enabled applications, DMF receives intensive attention and has been commercialized for newborn screening, SARS-Cov-2 diagnostics, high-throughput genomics *etc* [91]. The working mechanism for the conventional EWOD device is shown in Fig. 6a, where an electric potential is applied to the droplet and the electrode underneath for modifying the contact angle of the droplet. This device structure was further extended as a double-plate design as shown in Fig. 6b. In which the top electrode coated with a hydrophobic layer serves as a ground, the patterned electrodes at the bottom plate play a role for actuation. According to the mechanism of EWOD shown in Fig. 6a, if the patterned electrodes were connected with the electric signal asymmetrically, both CA and Laplace pressure difference will be induced to the left and right sides of the droplet, thus enabling a droplet actuation. By connecting the patterned electrodes sequentially, a continuous droplet actuation could be achieved. The droplet movement follows the sequence of electrodes connection. By fabricating the electrodes with a well-designed pattern and controlling the electric signals to the electrodes logically, the droplet could be actuated and merged for certain purposes. Fig. 6c shows a DMF platform targeting for single cell whole-genome sequencing [26]. Where the droplets were actuated for single cell isolation, merging with cell lysis solution and reaction for whole genome sequencing. DMF platforms with multi-functions are potentially employed for portable, fast-response and light-weight applications such as POC diagnosis. The bulky and expensive power sources as well as control circuit limit the wide spread of DMF platform. This section reviews the reported studies of employing TENGs with diverse working modes (single-electrode mode, contact-separation mode, free-standing mode) as a power source to actuate the droplet for DMF platform.

A TENG device working with the contact-separation mode was proposed as a power source for droplet actuation towards the self-powered DMF platform as shown in Fig. 7a. The TENG device was fabricated by electrospinning technology (Jiang et al. [115]) combining MXene nanosheet with poly(vinyl alcohol) (PVA) to enhance the output performance. The whole device shows a flexible feature with high output voltage. The TENG works stably and can reach a peak power density of 1087.6 mW/m^2 as the load resistance is 5.0 MΩ. By connecting the top and bottom aluminum electrodes to the copper electrodes of an EWOD device, the reciprocating motion of water droplets (2 μL, contained ink) on the four electrodes of EWOD was achieved. As an all-electrospun flexible power source, the TENG powered EWOD device shows great potential for harvesting the biomechanical energy from human motion for micro-scale drop manipulation towards a POC application. Apart from the contact-separation mode TENG driven EWOD devices, single-electrode mode TENG could also serve as a power source for droplet actuation on EWOD. Zheng et al. [112] built a TENG-driven droplet actuation system as shown in Fig. 7b. A

Please cite this article in press as: J. Tan et al., Materials Today, (2022), https://doi.org/10.1016/j.mattod.2022.07.009

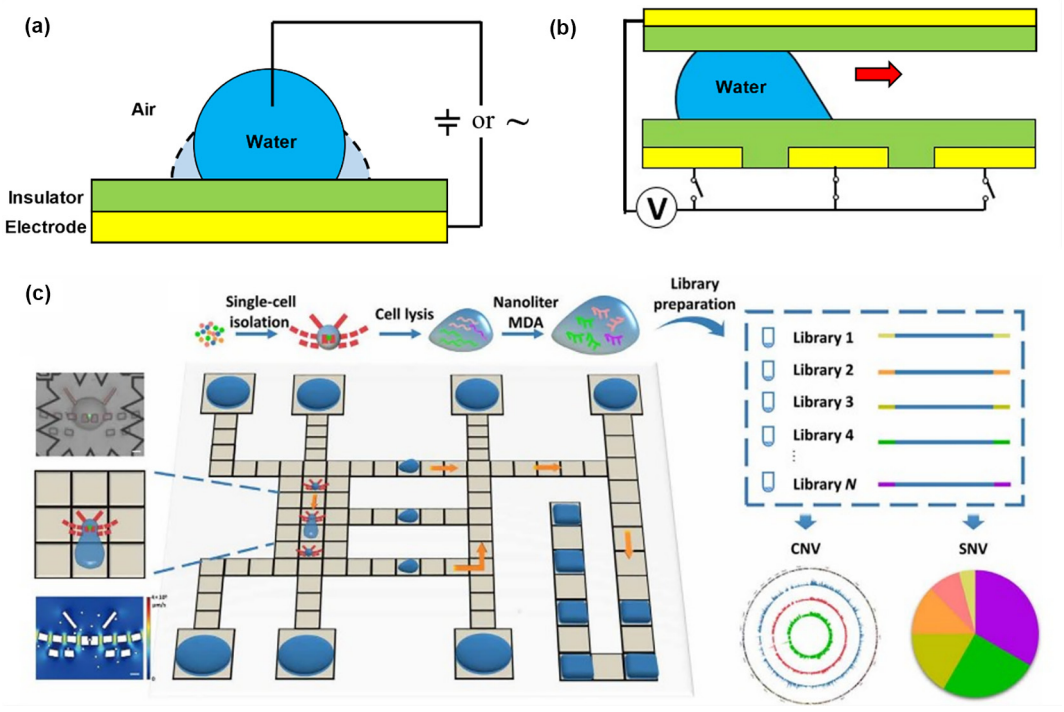

FIGURE 6

Schematic illustration of EWOD enabled digital microfluidics. (a) The contact angle of the droplet changes before (solid line) and after (dotted line) applying a voltage. (b) Schematic diagram of a typical DMF platform EWOD. (c) A DMF platform for single cells whole-genome sequencing, Reproduced with permission [88]. Copyright 2020, The American Association for the Advancement of Science.

single-electrode mode TENG was employed as the core element of the system, whereas the output voltage is generated by contact electrification between Kapton film and Aluminum foil. Two strip electrodes made of indium tin oxide (ITO) were placed underneath a superhydrophobic nanostructured fluorinated ethylene propylene (FEP) film to form a droplet actuation structure, where one electrode of EAS is grounded and the other electrode is connected to the single-electrode mode TENG. In order to increase the contact electrification, inductively coupled plasma (ICP) treatment was performed on Kapton film. For the electrical measurement of the TENG, the effective contact area of single electrode TENG is about 70 cm^2 (7 cm × 10 cm), while the applied pressure on the TENG is about 800 Pa. When the output voltage of TENG reaches 3500 V, the movement of the droplet can be realized. This large voltage (as compared to typical EWOD operation voltage e.g., tens to hundreds of volts) requirement is due to the fact that the actual voltage in EWOD device is much lower than the open-circuit voltage as the TENG also consumes part of the voltage ($V_{CD-pp}/V_{OC-pp} = 1/(1 + C_D/C_T)$), where V_{CD-pp} is the voltage on dielectric layer, V_{OC-pp} is the open-circuit voltage, C_D is the capacitance of liquid and C_T is the intrinsic capacitance of TENG [119]. This study also found that the changing of the droplet content (DI water, potassium hydroxide, phenolphthalein) would lead to different CA variations and driving distances with the same applied voltage. Chen et al. [92] employed a TENG device working with the freestanding mode to actuate droplets as a self-powered digital microfluidics (SP-DAS) platform. This study not only employs a freestanding working mode, but also utilizes sliding water drops to generate electricity on TENG. As shown in Fig. 7c, when one droplet is sliding along a tilted hydrophobic surface, the hydrophobic surface becomes negatively charged. The negatively charged surface will induce charge movement between electrodes which are patterned below the hydrophobic surface. A potential difference between the electrodes is generated. When the two electrodes are connected with another horizontally placed EWOD device, the induced potential difference modifies the CA of the droplet for actuation. The effects of sliding droplet size on the output voltage are investigated: the electrical energy generated by the sliding of a 60 μL droplet was able to trigger the movement of another 10 μL droplet horizontally, while the electrical energy generated by the sliding of a 40 μL droplet could only induce contact angle variation but not actuation. When the sliding droplet volume was increased to 80 μL, the increased EWOD force allowed to drive the droplet to climb to a larger inclination angle: 1 μL could climb to a surface with an inclination angle of α = 90°. Continuous droplet actuation and two droplets merging were demonstrated on the SP-DAS platform.

In addition to the TENG-powered EWOD droplet actuation, the researchers also developed more functional self-powered microfluidic platforms. Nie et al. [113] fabricated a freestanding mode TENG to drive a microfluidic platform and a mini vehicle on top of the driven droplets to transport tiny objects. The output voltage of TENG is generated by tribo-electrification between Kapton film and four Al foils, and inductively coupled plasma (ICP) treatment is performed on the Kapton film to obtain a larger surface charge density and increase the output performance of TENG. Hence, the surface of the Kapton film is covered with a pattern of nanostructures (Fig. 8a). The surface of the EWOD chip is a hydrophobic FEP film. In order to further

Please cite this article in press as: J. Tan et al., Materials Today, (2022), https://doi.org/10.1016/j.mattod.2022.07.009

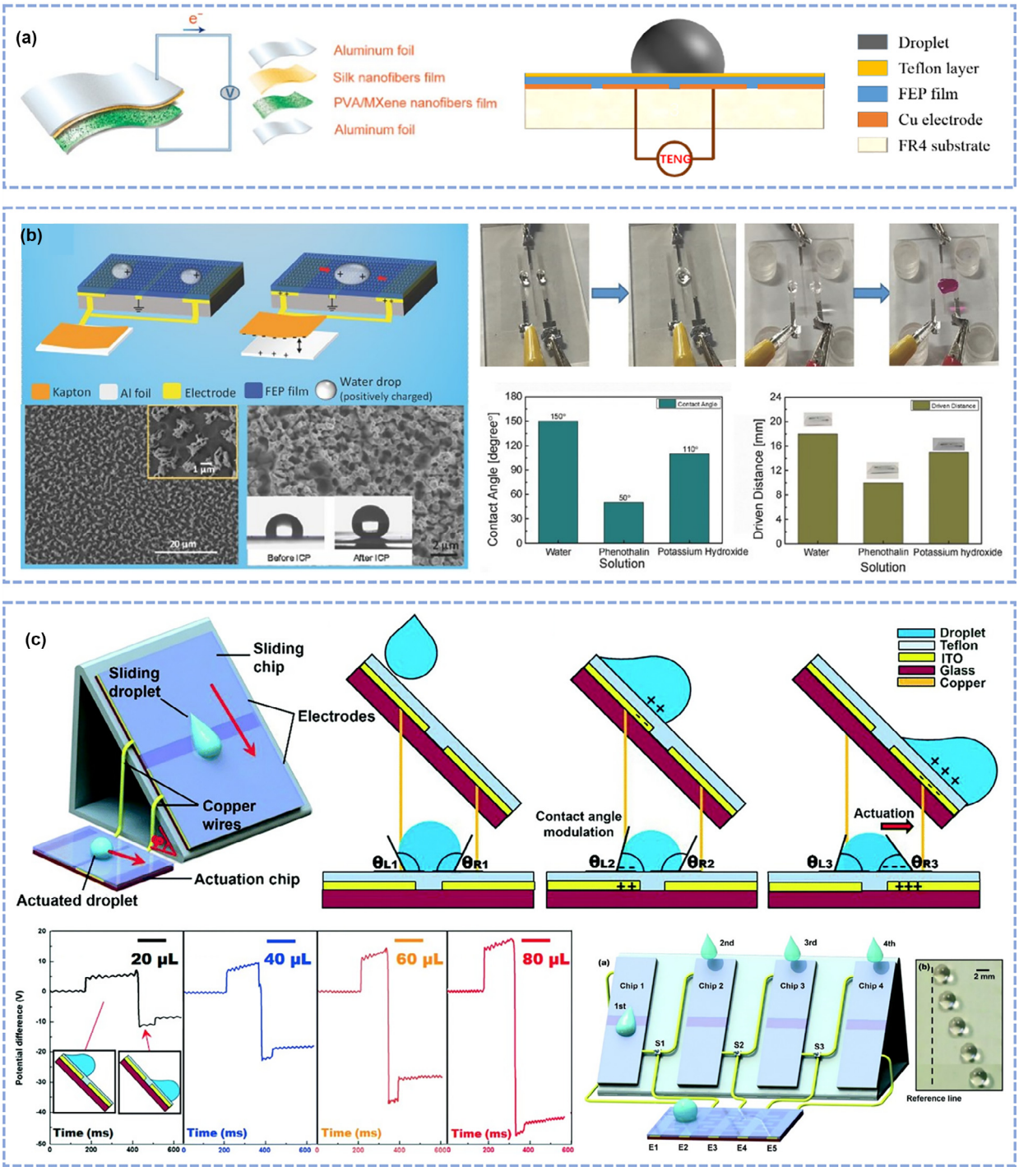

FIGURE 7

Applications of TENG powered droplet actuation system for DMF platform. (a) Schematic illustration of a contact-separation mode TENG powered droplet actuation device, Reproduced with permission [115]. Copyright 2019, Elsevier. (b) Schematic illustration of a single-electrode mode TENG powered droplet actuation system, Reproduced with permission [115]. Copyright 2017, Wiley-VCH. (c) Schematic illustration of a freestanding mode TENG powered droplet actuation system (SP-DAS), Reproduced with permission [92]. Copyright 2018, Royal Society of Chemistry.

improve the hydrophobicity, the surface of the FEP is chemically treated to increase the contact angle from 105° to 145°. The open-circuit voltage (V_{OC}) of this TENG is about 3500 V, the short-circuit current (I_{sc}) at a steady state is about 7.2 μA, and the maximum transferred charges are about 0.37 μC. The horizontal movement of droplets with a volume of 70 nL-5.0 μL driven by TENG was realized and the maximum driving distance is 25 mm. At the same time, the vertical driven of the droplet can also be realized as shown in Fig. 8a. Finally, by driving a small mini vehicle, the transportation of a maximum load of 500 mg was achieved. This work successfully realizes TENG-driven droplet manipulation (the minimum volume of the droplet can

Please cite this article in press as: J. Tan et al., Materials Today, (2022), https://doi.org/10.1016/j.mattod.2022.07.009

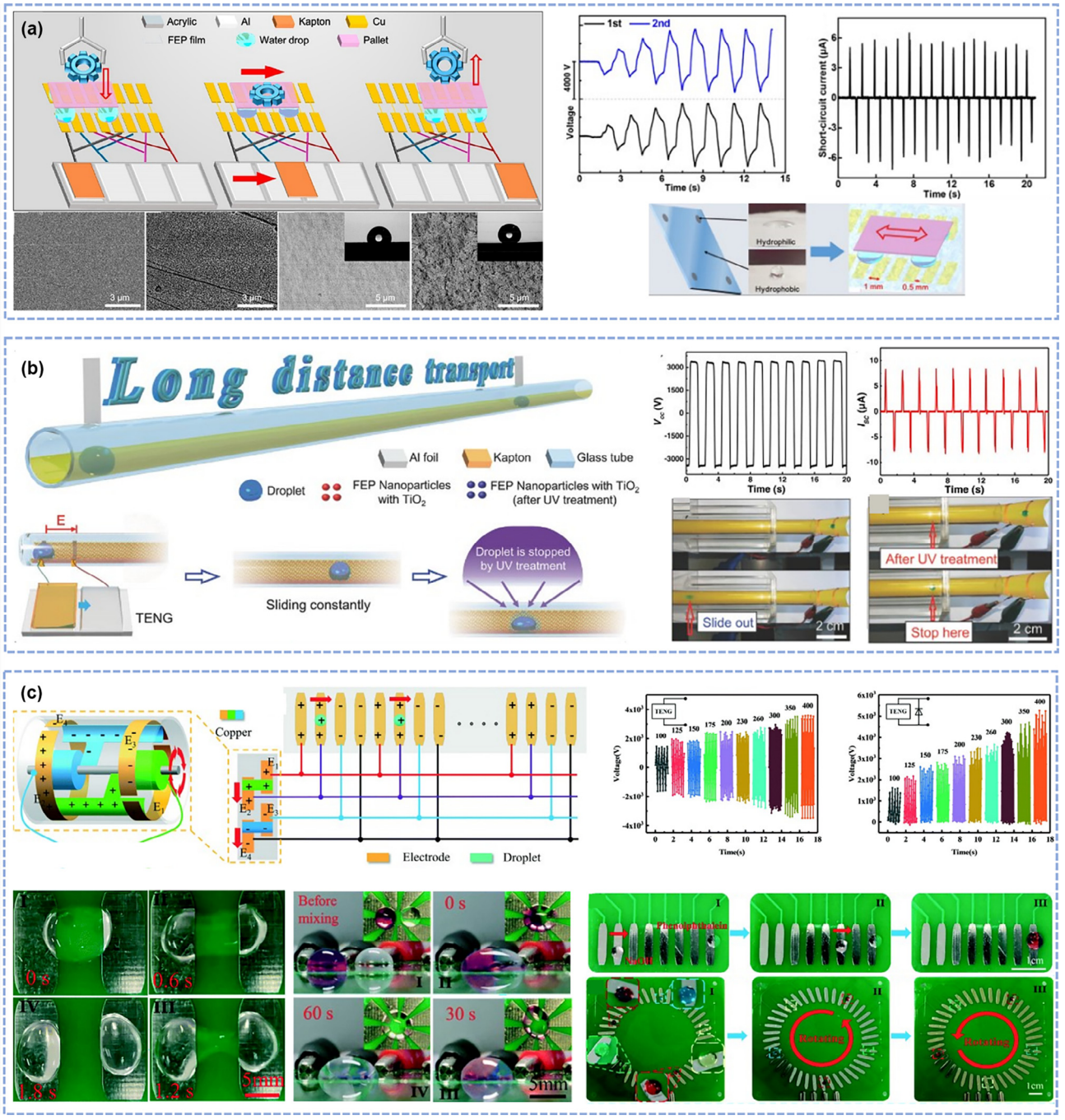

FIGURE 8

Applications of TENG powered droplet actuation system for DMF platform. (a) TENG driven droplet and object transportation. A maximum load of 500 mg and distance of 25 mm was achieved, Reproduced with permission [113]. Copyright 2018, American Chemical Society. (b) Schematic illustration of long distance ejected system based on TENG and PCAS, Reproduced with permission [114]. Copyright 2019, Wiley-VCH. (c) Schematic of a self-powered droplet manipulation system for transportation of droplets. The open-circuit voltage of the TENG versus time under different rotational speeds. Diverse droplet manipulation functions of splitting, mixing and transportation were achieved on the TENG driven DMF platform, Reproduced with permission [116]. Copyright 2021, Royal Society of Chemistry.

reach 70–80 nL) and the tiny object by a mini vehicle on top of the droplets. It provides a new idea for self-driven digital microfluidic transport system. A smart microfluidic system driven by TENG proposed by Nie et al., [114] realizes driving of droplets through photo-controllable method in a given position (Fig. 8b). A freestanding TENG is prepared and employed as the driving source of this microfluidic system, where the materials for contact electrification are Kapton film and Al foils. Two electrodes connected to two Al foils of TENG are pasted to the outer wall of the quartz glass tube. Therefore, the sliding motion of the Kapton film between two Al foils can induce a strong electric field between the two electrodes for generating a large electrostatic force on the water droplet. The open-circuit voltage (V_{oc}) and short-circuit current (I_{sc}) of the freestanding TENG reach

Please cite this article in press as: J. Tan et al., Materials Today, (2022), https://doi.org/10.1016/j.mattod.2022.07.009

peak values of 3400 V and 8.5 μA, respectively. For this smart microfluidic system, by combining TENG with photo-controllable adhesion surfaces (PCAS), microdroplets are ejected for long distances in a quartz glass tube, while UV light can accurately capture water droplets at a given position. The PCAS is obtained by sputtering a photo-response material, such as TiO_2 onto the FEP surface. The water CA of the prepared PCAS surface is about 161.5° (store in the dark) and 91.2° (after UV irradiation for 20 min), and this process is reversible. Then, the long-distance transportation of droplets in the tube is realized, the maximized ejecting distance reaches 620 mm and the maximized instantaneous velocity exceeds 0.5 m s^{-1}. This study employs electrostatic force for droplet actuation which requires a large operating voltage. The working mechanism is different from EWOD and provides a new idea for TENG-driven droplet microfluidics, as well as a wide variety of potential applications, including inkjet printing, localized chemical reactor, drug/cell delivery on microscale, and so on.

The above work has made the foundation for the self-powered droplet actuation and achieved remarkable results. However, realizing self-powered digital microfluidics also requires more functions including droplet dispense, mixing, and splitting. Yu et al. [116] proposed a self-powered droplet manipulation system (SDMS) to realize various droplet operations, including moving, splitting, merging, mixing, transporting chemicals and reacting (Fig. 8c). It mainly includes a rotating freestanding triboelectric nanogenerator with an electric brush (EB-TENG) and a DMF device. Diverse functions of droplet manipulation can be achieved on this self-powered DMF platform. As the transportation, merging and splitting require different threshold voltages, the EB-TENG utilizes a design with different electric brushes. By connecting different brushes to the DMF platform, variable open-circuit voltage could be attained for different functions accordingly. The TENG consists of a cylindrical stator and a rotor. Contact electrification is generated between the polytetrafluoroethylene (PTFE) film of the rotor and the nylon film of the stator, and the copper foils serve as the electrodes. The output voltage of TENG increases with the increase of rotational speed (from 1400 to 3500 V as the rotation speed increases from 100 to 400 r min^{-1}). The volume of the droplet that can be driven on this platform varies from 1.4 to 500 μL. This large operation range allows for diverse applications on the DMF platform. The moving velocity of the droplets varies from 10.6 to 45 mm/s when the electrode width increases from 0.5 to 4.5 mm and the gap is fixed as 2 mm. By using TENG and dielectrophoretic (DEP) force, the self-powered system realizes various droplet operations, including moving, splitting, merging, mixing, transporting chemicals and reacting.

In conclusion, the EWOD-based DMF technology powered by TENG can get rid of the traditional bulky power supply. The droplets are driven by external mechanical stimuli complete the delivery of chemicals for chemical reactions. Based on this technology, different potential applications can be developed, including chemical delivery, biochemical analysis and wearable sensors. Of course, more research is still needed to advance the technology, including integration of self-powered devices, electric circuit design, multiple electrodes control as well as the optimization of materials and structures.

EWOD based optical devices driven by TENG

Apart from the droplet actuation and DMF platforms, another major application of EWOD is for optical devices, including micro-lenses [122–125], fiber optics [126,127] and display technology [128–132]. Fig. 9 shows the working principle of the EWOD display device (a) and EWOD based lenses (b). As for the display device, the top and bottom plates are filled with immiscible water and oil. As the solid/water interfacial tension is greater than solid/oil, the dyed oil droplet spreads on the hydrophobic surface initially. When an electric potential is applied between the water and the electrode underneath the hydrophobic coating, the water spreads and squeezes the oil droplet to a side, allowing for the light transmission from the bot-

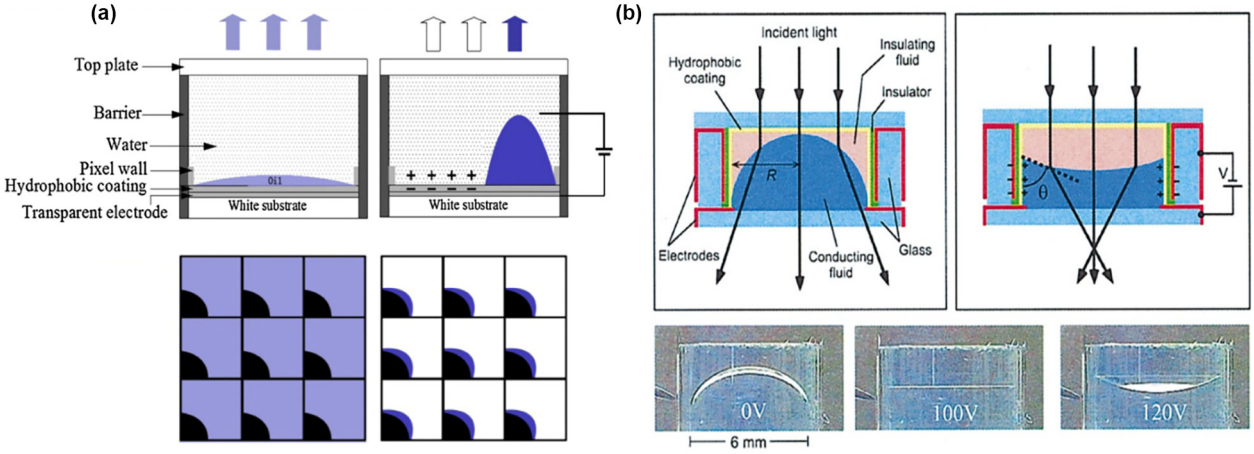

FIGURE 9

Schematic illustration of EWOD based optical devices. (a) An EWOD display screen enables renderings when the oil comes out (zero electric potential) and transparent when the oil is pushed aside (high electric potential), Reproduced with permission [134]. Copyright 2015, Elsevier. (b) Schematic of EWOD based tunable lenses. When voltages of different magnitudes are applied to the water in the middle and the EWOD side walls, the prisms exhibit different liquid surface shapes for beam steering, Reproduced with permission [90]. Copyright 2004, American Institute of Physics.

Please cite this article in press as: J. Tan et al., Materials Today, (2022), https://doi.org/10.1016/j.mattod.2022.07.009

tom to the top. By patterning the electrodes and water/oil array, EWOD enabled display could be realized. In terms of liquid lenses as shown in Fig. 9b, the EWOD devices are built as side walls of a container. When injecting density matching immiscible water and oil phases into the container, the droplet would show a superhydrophobic CA on the side walls due to the greater solid/water interfacial tension, as compared to the solid/oil. Similarly, when an electric potential is applied between the water droplet and the side walls, the droplet would spread to the solid surface, together with the functions of oil/water interfacial tension, diverse shapes (*e.g.*, rectangle, trapezoid and inverse trapezoid) of water could be achieved. Since the refractive indices of the oil and water are different, the shape change of the water phase could change the light path shining on the device. According to the requirement of diverse applications, the water shape change could be employed for focal length control, beam steering, dynamic total internal reflection (TIF). As compared to the conventional solid glass made optical devices, the EWOD enabled optical devices to provide benefits of dynamic control and low power consumption. This technology has been commercialized by de Laclarée *etc*. However, the high voltage required for EWOD device operation presents challenges in terms of power consumption and safety. TENG could be employed as a high-voltage power supply for driving the optical devices [133]. The TENG based power supply is attractive for outdoor display applications where the electrical connection is difficult. This section reviews the devices on the TENG-driven EWOD based optical devices.

Li et al. [95] designed a flexible TENG to drive an EWOD display device as shown in Fig. 10a. This TENG device was fabricated by the direct ink writing (DIW) method. This study selected fast-curing silicone elastomer as viscoelastic inks as material for contact electrification. The TENG device works in the vertical contact-separation mode and has an open-circuit voltage of up to 124 V and a maximum power density of 608.5 mW/m^2. Moreover, EWOD based display was tested with

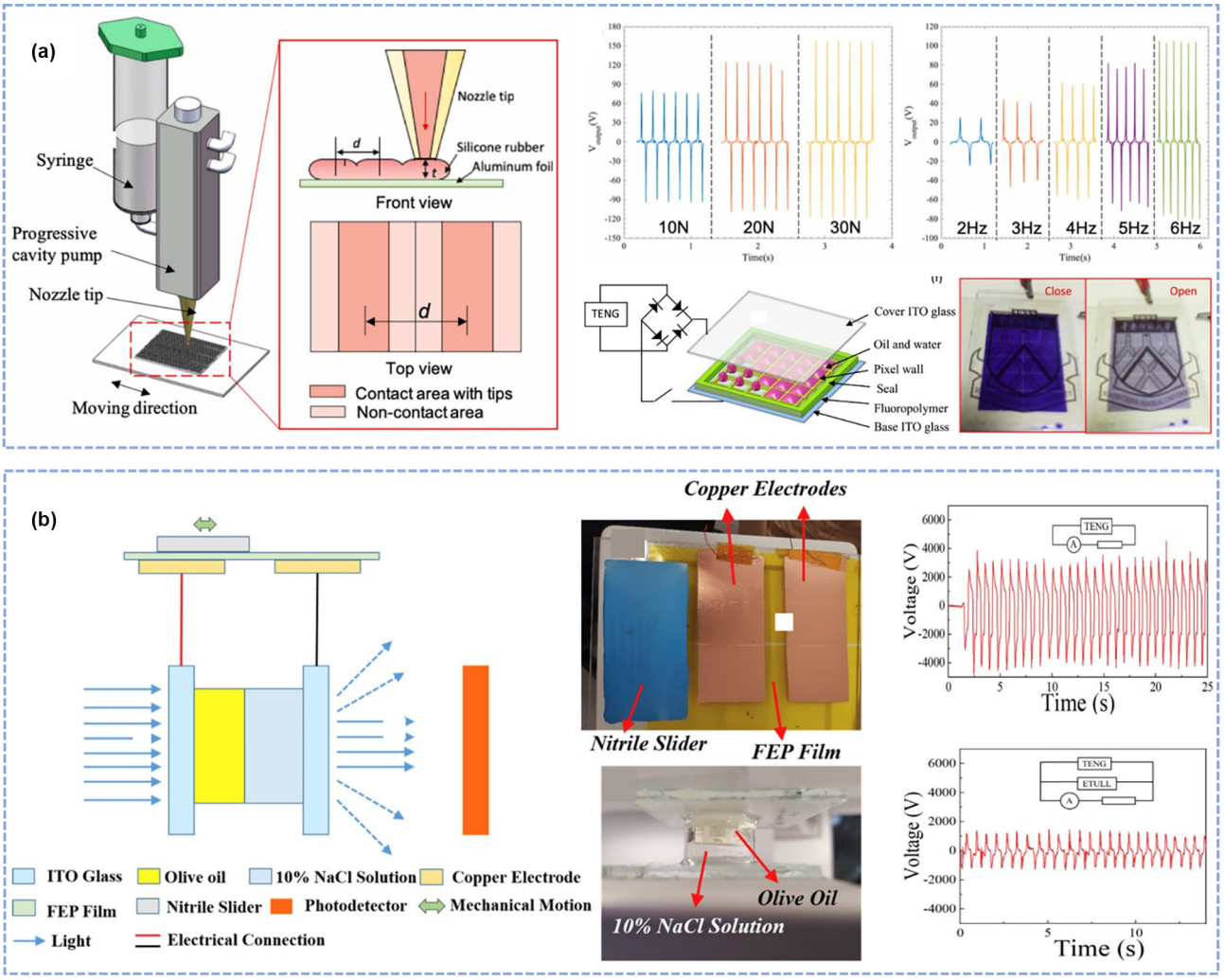

FIGURE 10

Applications of TENG powered tunable lenses. (a) 3D printed flexible triboelectric nanogenerator for EWOD display, Reproduced with permission [95]. Copyright 2019, Elsevier. (b) Schematic illustration of the self-powered EOS comprised of a FS-TENG and an ETULL. The interfacial curvature of the two liquids can be changed upon loading the triboelectrification induced voltage, enabling the remote sensing function, Reproduced with permission [117]. Copyright 2019, Elsevier.

Please cite this article in press as: J. Tan et al., Materials Today, (2022), https://doi.org/10.1016/j.mattod.2022.07.009

the output voltage of TENG. A full-wave rectifier was used to convert the alternating current generated by the TENG into a direct-current signal. When the applied voltage can trigger EWOD phenomenon, the blue oil inside the EWOD display device shrinks to the corners of the pixels. At this time, the color of EWOD will switch quickly, and the logo at the bottom can be clearly seen. The above results indicate that TENG has excellent potential in wearable electronic displays, mainly when both TENG and EWOD devices are fabricated flexibly.

Wang et al. [117] proposed a self-powered EWOD optical switch (EOS) by a combination of a freestanding sliding mode triboelectric nanogenerator (FS-TENG) and an electrically tunable liquid lens (ETULL) as shown in Fig. 10b. In this device, nitrile and fluorinated ethylene propylene (FEP) film were chosen as materials for triboelectrification. The device was fabricated with a size of 7 cm × 14 cm. The ETULL was fabricated by a conducting fluid, an insulating oil and an acrylic cylindrical spacer as well as two indium tin oxide (ITO) electrodes. The peak open-circuit voltage of the FS-TENG reaches 3500 V and the voltage drop of the ETULL is 1100 V. The measurement results illustrate that the capacitance of the ETULL is around twice that of TENG. Upon applying a voltage to the ETULL, the interface between two liquids was bent due to the electrostatic force, forming an insulating oil-based concave lens. Notably, this device structure is different from that shown in Fig. 9b. This is because the electrode for applying the electrostatic force was built on the top and bottom walls of the ETULL, instead of on the side walls as shown in Fig. 9b. Driven by the electrostatic force generated by the high voltage of TENG, an insulating oil-based concave lens with a maximum aspect ratio of 0.25 can be realized, which could be employed for diverging the incident light. To verify the effectiveness of the proposed self-powered EOS, a wireless sensing system was built by the TENG powered ETULL system: when mechanical energy (*e.g.,* suspicious intrusion) is applied to the TENG, the generated voltage will trigger the ETULL for incident laser beam diverging. The divergence of the laser beam could be employed to trigger an alarm. This electromechanical optical signal conversion realizes wireless sensing and can be applied to various fields such as human machine interface, remote monitoring of infrastructure health, security detection, and wireless smart keyboard.

Chen et al. [93] proposed a programmable compound prism (PCP) powered by TENG for solar beam steering (Fig. 11a). By employing a freestanding mode TENG made of FEP and copper electrodes, the TENG could generate an open-circuit voltage of up to 530 V (peak-to-peak signal). The output of TENG was connected with an RC circuit for converting the AC signal into a DC signal. By changing the resistance of the RC circuit, variable DC output signals could be obtained for triggering the EWOD based PCP. The PCP was fabricated with two pieces of EWOD glass (glass substrate coated with ITO electrode and Teflon hydrophobic layer) and two pieces of bare glass to form a container. The PCP was filled with DC 550 silicone oil, DI water and PMX 200 silicone oil, due to density matching, the DI water maintains stability between the DC 550 silicone oil and the PMX 200 silicone oil. When connecting the variable DC signals from the TENG and RC circuit to the side walls and DI water in the PCP, the water shape could be modulated in a programmable manner. The shape of water was modulated as a trapezoid, rectangle, and inverse trapezoid as shown in Fig. 11b. As the three immiscible liquids possess different refractive indices to the incident light, the light path could be deflected during the shape change of water. A maximum deflection angle range of 15° was achieved in the TENG powered PCP, which is 38% greater than conventional single prism with one pair of oil/water interface. The programmable light deflection property of the TENG powered PCP could be employed for solar beam steering in concentration PV applications: when the incident light beams are from different orientations in the morning and afternoon, the PCP could change its prism angle to deflect the light beam perpendicularly. The proposed TENG-PCP was demonstrated to deflect an oblique incident laser beam, and the perpendicular outgoing beam successfully spots the multi-junction solar cell to boost the output power from 0.088 mW to 1.288 mW by solar cell.

Fang et al. [118] developed a varifocal liquid lens based on TENG (TVLL). The basic structure of the TVLL consists of a freestanding-mode TENG and a varifocal liquid lens with a sandwich structure, in which the two electrodes of the TENG are directly connected to the upper and lower electrodes of the liquid lens (Fig. 11c). The liquid lens chamber's length, width, and height are 10, 10, and 1 mm, respectively. Copper and fluorinated ethylene propylene (FEP) were selected as contact electrification materials. At the same time, in order to strengthen the output performance of TENG, the FEP films were inductively coupled plasma (ICP) treated. The open-circuit voltage (V_{OC}) basically increases linearly from 0 to 7 kV as the sliding distance of the TENG changes (0–180 mm). For the liquid lens, polyphenylmethylsiloxane (PMSO) was selected as the optical medium due to its unique attributes, such as a high transmittance (over 90% to visible light), a slow evaporation rate, low viscous resistance and excellent electrical insulation performance. When a voltage is applied, a pressure difference is created inside the liquid lens of $\Delta P_S = \sigma\kappa$, where ΔP_S is the pressure difference, σ is the surface tension between air and the liquid, and κ is the curvature of the air–liquid interface. The performance of the proposed TVLL is investigated in detail for different structural parameters; when the electrode height/width ratio is 0.1 and the volume of the optical medium in the liquid lens is 20 μL, the focal length is modulated from −6 mm to infinity to 7 mm by sliding the TENG. Furthermore, based on the precise modulation effect of the TVLL on the beam, a triboelectric magnifier is demonstrated, in which the magnification can be directly modulated by sliding the triboelectric layer of the TENG. The TENG powered TVLL was further demonstrated to change the focal point of a laser beam.

In conclusion, the EWOD optical device powered by TENG is mainly for research in display and tunable lens devices. The researchers fabricated TENGs with diverse working modes to trigger the EWOD effect to drive different optical devices for beam steering in concentration photovoltaics, zoom lenses, magnifying glasses, display *etc.* EWOD optical devices powered by TENG can realize the independence from traditional high voltage power supply, which is favorable in outdoor self-powered light tracking, self-powered display, etc. The results shown above prove that TENG-powered EWOD optics have broad application scenarios. Furthermore, with the improvement of material prop-

Please cite this article in press as: J. Tan et al., Materials Today, (2022), https://doi.org/10.1016/j.mattod.2022.07.009

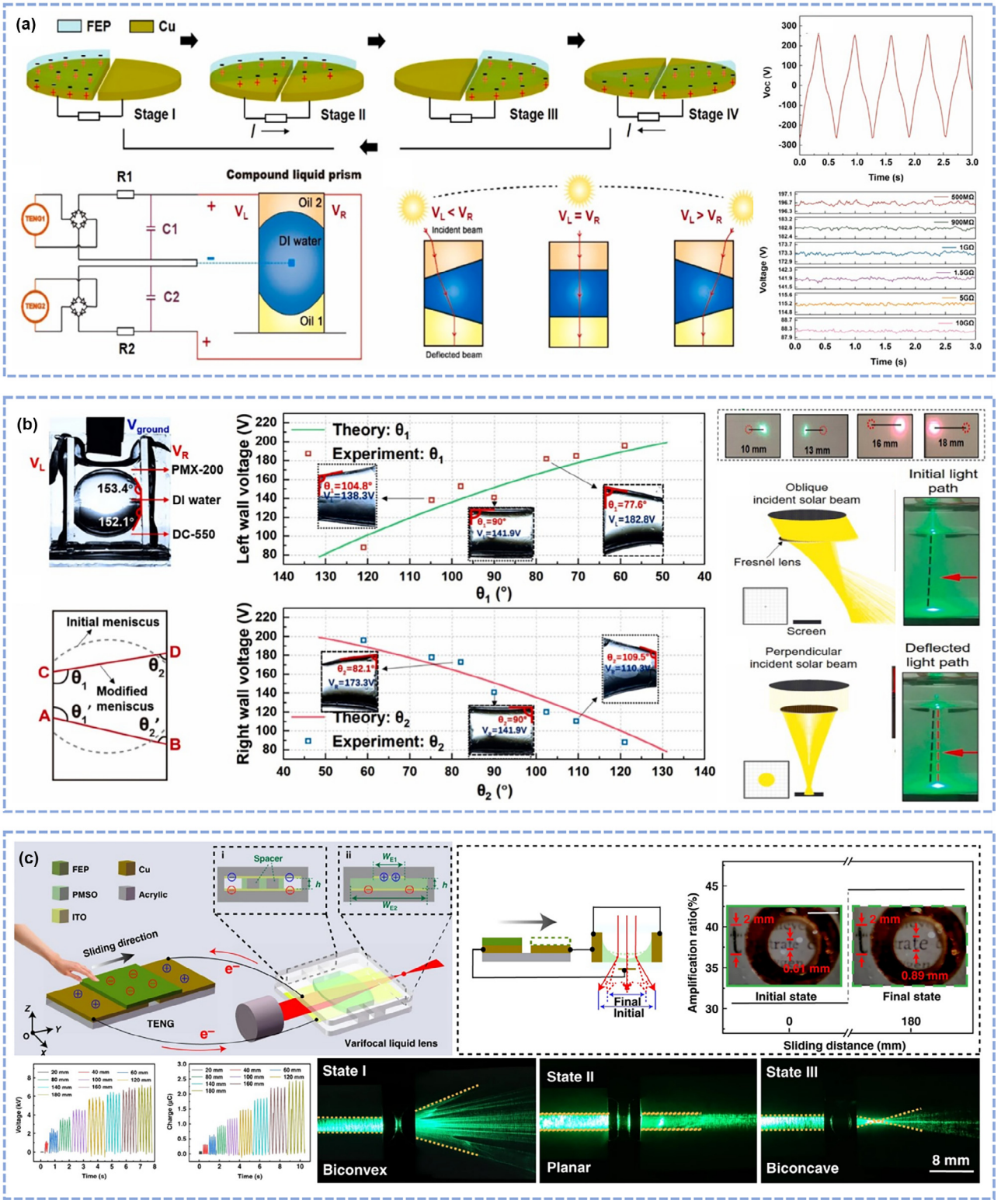

FIGURE 11

Applications of TENG powered tunable lenses. (a) Concept of the TENG-PCP beam steering system for concentrator photovoltaics (CPV) applications. The output of TENG could be rectified and employed for modulating the oil/water/oil interfaces in the prism for beam steering, Reproduced with permission [93]. Copyright 2021, Elsevier. (b) The output performance of TENG and DC voltage signal on the PCP varying with the resistance of the RC circuit. Beam deflection under TENG-PCP, Reproduced with permission [93]. Copyright 2021, Elsevier. (c) Performance of a TENG powered varifocal liquid lens (TVLL), Reproduced with permission [118]. Copyright 2020, Nature Publishing Group.

Please cite this article in press as: J. Tan et al., Materials Today, (2022), https://doi.org/10.1016/j.mattod.2022.07.009

erties, TENG is expected to achieve larger output in a smaller size [135], thus enabling the development and application of small-scale, wearable and self-powered optical devices.

EWOD based emerging technologies driven by TENG

With the advantages of EWOD technology in microscale liquid handling and the benefits of simple fabrication and low power consumption, EWOD technology has also been applied to diverse emerging technologies [136,137]. These technologies could be classified into four categories, including the EWOD phenomenon based anti-fogging, microfluidic valve, EWOD enabled capillary propeller and other emerging technologies. The schematics of the EWOD based droplet coalescence and anti-fogging device are shown in Fig. 12a [138,139]. A planar EWOD device with patterned electrodes is covered with randomly distributed tiny droplets (fog drops). When an AC electric signal is connected with the neighboring electrodes, the EWOD phenomenon is triggered and the wetting condition of the droplets varies from hydrophobic to hydrophilic with time. During the spreading process, the neighboring droplets easily coalesce and form a larger merged droplet. When the merged droplet is great enough, the droplet will slide off the glass with a greater gravitational force as compared to the drag force. Bahadur et al. [140] showed that heat transfer performance of condensed droplets was significantly improved based on the AC EWOD induced droplet coalescence and shedding. As shown in Fig. 12b, the device could be employed as a valve when the EWOD phenomenon is applied to a dielectric and hydrophobic material coated metal mesh substrate. The droplet on top of the device stays above the mesh EWOD substrate as the mesh size is delicate enough without an electric potential. When an electric potential is applied between the droplet and the hydrophobic coated mesh, the wetting condition changes from hydrophobic to hydrophilic and the droplet could penetrate to the bottom of the device. This phenomenon enables the mesh EWOD device as a controllable valve for microfluidic applications. Ainla et al. [89] used the principle of EWOD to realize a high-speed response valve, which requires low energy (~27 μJ per actuation), and works with various aqueous solutions. As shown in Fig. 12c, the EWOD phenomenon was employed for capillary propulsion of floating objects. This configuration of EWOD device was achieved by inserting an EWOD chip into a pool of water. The bulk water in the pool serves as the droplet in a conventional EWOD configuration. When inserting an EWOD chip to the water pool, the contact line shows a hydrophobic wetting condition without an electric potential. When a high electric potential is applied between the EWOD chip and the water, the wetting condition changes and the contact line rises accordingly. When an AC electric signal is applied, the contact line oscillates between hydrophobic and hydrophilic conditions, leading to the formation of a capillary wave at the air/water interface. The propagation of the capillary wave would apply a reaction force to the EWOD chip which could be employed for propelling tiny floating objects. This capillary propeller was proposed by Yuan et al. [141] for propelling a light-weight boat on the water surface. The EWOD based capillary wave propeller was further demonstrated with functions of wireless propulsion [142] and large amplitude curved propulsion [143]. These emerging EWOD devices also require an external power source, so the research on emerging EWOD devices powered by TENG are carried out accordingly. This section will review the TENG-powered EWOD devices for three emerging technologies including anti-fogging, EWOD valve and capillary propeller.

Anti-fogging technology

In order to eliminate the high voltage power source requirement in EWOD based anti-fogging applications, Tan et al. [96]. proposed a method of using rotating TENG (RF-TENG) which is capable of converting arbitrary mechanical energy into electricity to drive an EWOD device to achieve anti-fogging purpose (Fig. 13a). The materials for contact electrification are fluorinated ethylene propylene (FEP) and nylon due to their high surface charge density. The RF-TENG could generate variable open-circuit voltage (0.73–5.26 kV) and frequency (20–100 Hz) by changing the contact area and the rotating speed of the rotor. EWOD anti-fogging glass consists of interdigitated electrodes and a Teflon hydrophobic layer. In the experiment, the mechanism of droplet coalescence under AC EWOD was analyzed through the images

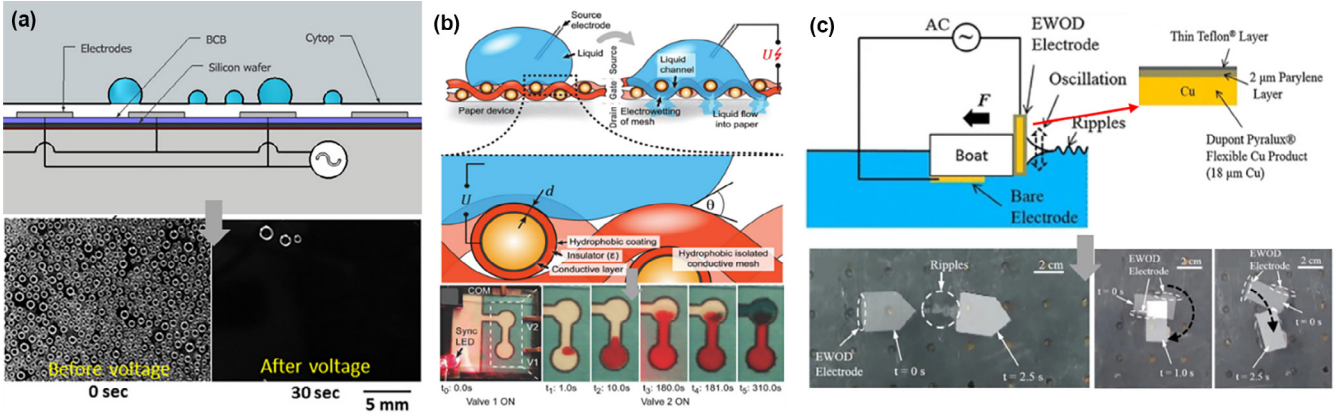

FIGURE 12

Schematic of EWOD enabled emerging technologies. (a) Schematic diagram of the EWOD enabled droplet coalescence and anti-fogging, Reproduced with permission [139]. Copyright 2020, American Institute of Physics. (b) Working principle of an EWOD valve, Reproduced with permission [89]. Copyright 2017, Wiley-VCH. (c) Schematic of an EWOD enabled capillary wave propeller, Reproduced with permission [141]. Copyright 2015, Springer.

Please cite this article in press as: J. Tan et al., Materials Today, (2022), https://doi.org/10.1016/j.mattod.2022.07.009

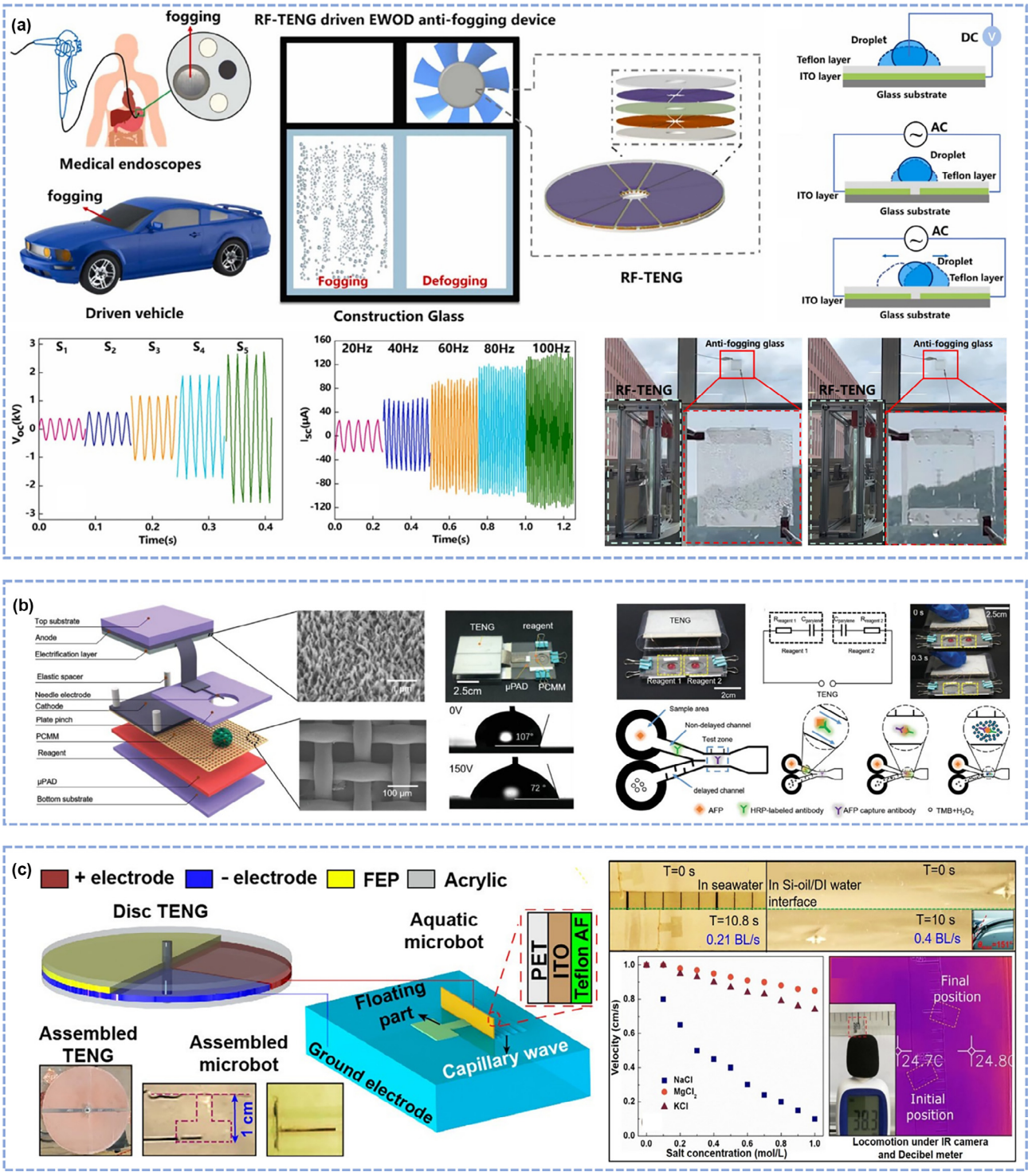

FIGURE 13

Applications of TENG powered EWOD based emerging technologies. (a) Schematic and performance of a TENG powered AC EWOD anti-fogging glass. When external mechanical energy (*e.g.,* wind) is converted into electric potential by RF-TENG, the fog droplets on the AC EWOD glass coalescence and shed off. Reproduced with permission [96]. Copyright 2022, Elsevier. (b) A self-powered EWOD valve (SPEV) driven by an energy-harvesting triboelectric nanogenerator (TENG), Reproduced with permission [97]. Copyright 2019, Wiley-VCH. (c) Concept of the aquatic TENG-Bot. The aquatic TENG-Bot is composed of a disc TENG and one EWA. During operation, the rotation of the disc TENG transfers charges to the actuator and ground electrodes alternatively and generates capillary waves for actuation, Reproduced with permission [94]. Copyright 2020, American Chemical Society.

captured by a high-speed camera. The spreading and lateral movement of droplets were triggered by the output signal from RF-TENG. The coalescence and lateral movement of the droplets enable merging and sliding down of the merged droplets to achieve anti-fogging performance. The experimental results show that when the open-circuit voltage is greater than ± 1 kV

Please cite this article in press as: J. Tan et al., Materials Today, (2022), https://doi.org/10.1016/j.mattod.2022.07.009

and a frequency larger than 60 Hz is able to achieve a large dry area fraction from 34% to 98% in a very short time (<0.5 s). In order to characterize the light transmittance of the EWOD anti-fogging glass, two samples were tested for transmittance. The results indicate that the EWOD glass show a good visible light transmittance, only 3% lower than the ordinary glass. For practical demonstration, the device was attached to the window of a laboratory. The results show that the device could remove water fogging on a laboratory window, allowing for the observation of the vision outside by the TENG driven anti-fogging. Besides, the devices achieved continuous anti-fogging performance for repeated cycles. The TENG powered EWOD anti-fogging glass shows superior features such as extremely fast response time, good durability and no heat generation, as compared to the conventional hot wind and hydrophilic patterning methods. This study paves the way for utilizing renewable mechanical energy (e.g., wind) for indoor anti-fogging.

EWOD based valve

Microfluidics and the miniaturization of biosensors have gained increased interest as analytical tools for medical diagnostics, [144] drug delivery, [145,146] and synthesis and biological applications [147]. These devices rely on a valve for effective flow control in microscale channels. The EWOD based valve combined with the plasma-modified Teflon microfluidic guidance in controlling continuous fluid flow has been demonstrated [148]. Since then, this technology has been studied intensively (*e.g.*, Satoh et al. [149]). However, most of the previously reported EWOD valves are usually triggered by an externally supplied voltage source of several hundreds of volts [150,151]. This limitation is a key challenge in developing portable, compact and all-in-one EWOD valves. In this context, Guo et al. [97] developed a self-powered EWOD valve (SPEV) for precisely driving paper-based microfluidic analysis, which is enabled by an energy-harvesting TENG (Fig. 13b). They fabricated a TENG in contact separation mode, which outputs a voltage of 380 V by collecting external mechanical energy (much higher than the actuation voltage of the SPEV ~130 V). The structure of the EWOD valve is shown in Fig. 13b. Once actuated, the EW valve can be instantly switched on at a response time of 0.18 s, allowing liquid reagent to flow through the valve. The SPEV can be used for simultaneous addition of multiple reagents in an enzyme-linked immunosorbent assay on a paper-based microfluidic analytical device (μPAD). This SPEV has the advantages of low cost, simple operability, high response speed. Combining with μPADs, the SPEV is suitable to be used in many other complex multi-procedure assays, including enzyme linked immune sorbent assay (ELISA), electrochemiluminescence (ECL), DNA detection, water quality, environmental monitoring, *etc.*

Capillary propeller

It is known that DC triggered EWOD could modify the wetting of aqueous solution from hydrophobic to hydrophilic constantly. On the other hand, the pulsed or AC electric signal could realize the oscillation of droplets periodically [152,153]. Apart from droplet, the AC EWOD could induce oscillation of the contact line of bulk water when an EWOD device is inserted. Mita et al. [154] and Yuan et al. [141] proposed the AC EWOD capillary propeller. Similarly, this small capillary propeller also requires an external power supply to drive. To address the above problems, Jiang et al. [94] present a TENG powered EWOD actuator (TENG-EWA) for aquatic microbots: the aquatic TENG-Bot (Fig. 13c). The aquatic TENG-Bot consists of one freestanding mode disc TENG, a floating part, and an EWOD actuator (EWA). The TENG consists of a pair of copper electrodes thermally deposited on an acrylic substrate, a commercial FEP (fluorinated ethylene and propylene) film, and an acrylic cover. The EWA is composed of a spin-coated and cured Teflon AF solution, a wet-etched ITO (indium tin oxide)-coated PET sheet, and connection wires. When TENG starts to work, the transferred tribocharges of a disc TENG alternatively modify the surface energy of the EWOD actuator, yielding a capillary wave propagation. The reaction force of the capillary wave actuates the microbot on the water surface. An optical transparent microbot (weight of 0.07 g, body length of 1 cm) was actuated forward at a maximum locomotion velocity of 1 cm/s. The proposed aquatic TENG-Bot not only shows the potential of converting environmental energy into actuation force for microbots but also reveals advantages in optical, sonic, and infrared concealment.

Other applications of TENG powered EWOD devices

In addition, the TENG-driven EWOD droplet control also provides a new idea in the research of human wearable sensors. Shen et al. [120] developed a wearable EWOD medium sensor for real-time human sweat monitoring (Fig. 14a). Using TENG to collect the mechanical energy of human motion, convert it into electrical energy to power the EWOD device, and realize self-driven human sweat collection and detection. The results of this study demonstrate the application prospects of TENG-driven EWOD devices in wearable self-powered devices. With the further improvement of TENG technology, more self-powered wearable devices are expected to be developed. EWOD is a versatile technique for controlling the liquid-wetting behavior of solid surfaces. Furthermore, Wang et al. [119] recently developed a TENG-powered EWOD device that enables self-powered electrocapillary filling and micro-molding, which allows for fabricating the originally difficult-to-mold micro-structures in a handy way (Fig. 14b). However, in the process of micro-machining, how to realize the continuous and stable energy supply and precision control of TENG. Compared with the traditional power source, using TENG for EWOD micromachining, the advantages need to be further verified. The above works expand the application scope of TENG-driven EWOD devices. With the deepening of research, more miniaturized, self-powered and wearable devices will be developed and applied.

In conclusion, the above-mentioned emerging TENG-powered EWOD technology greatly expands the application scenarios of this technology. The use of TENG power supplies can free these emerging technologies from the dependence on traditional bulky power supplies, broadening the scope of these applications. The above work has confirmed that TENG-powered EWOD devices can be applied to anti-fogging, EWOD valves, capillary propeller, microfabrication and wearable sensor. Since these technologies have just been developed, much in-depth research is needed, including energy transfer control, optimiza-

Please cite this article in press as: J. Tan et al., Materials Today, (2022), https://doi.org/10.1016/j.mattod.2022.07.009

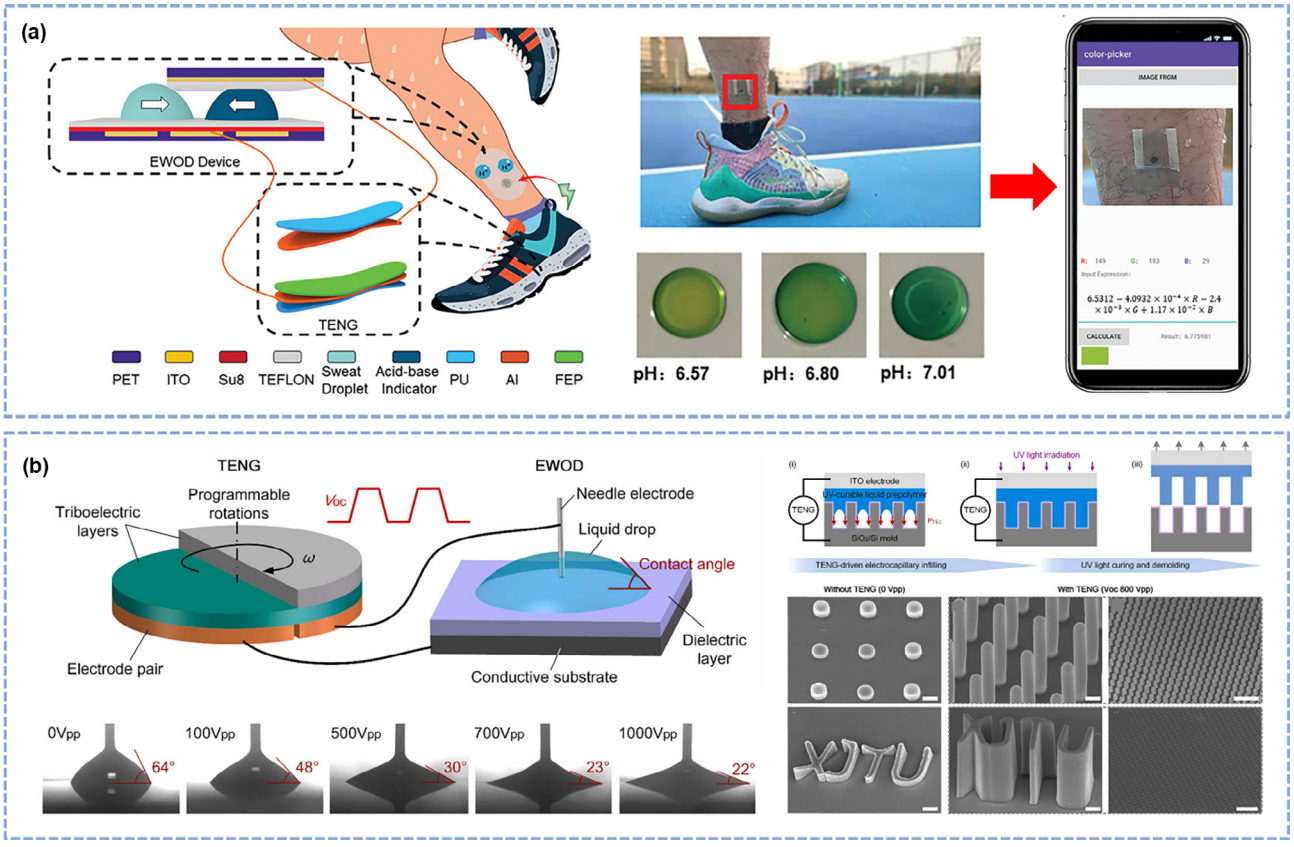

FIGURE 14

(a) Schematic illustration of a wearable droplet-based human sweat monitoring platform (WSMP) powered by TENG, Reproduced with permission [120]. Copyright 2022, Wiley-VCH. (b) Schematic illustration of the self-powered electrocapillary infilling and micromolding for fabricating microstructures, Reproduced with permission [119]. Copyright 2022, Elsevier.

tion of materials and structures and expansion of application scenarios.

Summary and perspectives

In summary, recent advances in TENG powered EWOD devices are systematically reviewed. It is seen that the TENG with single-electrode, contact separation and freestanding working modes are all suitable for driving the EWOD devices. As for the EWOD devices, diverse applications including digital microfluidics, tunable lenses, electronic display, anti-fogging device, EWOD valve, and capillary propulsion have been demonstrated to be powered by TENG. The combination of the two technologies not only eliminates the requirement on high-voltage power sources for EWOD, but also opens up opportunities towards the self-powered liquid actuators for more applications. In recent years, the rapid development of TENG technology has boosted the research and development on self-powered sensors, the TENG driven self-powered liquid actuators are promising for more in-depth investigation. Since actuators play important roles in robotics, optics, space technology (surface tension dominated in microgravity environment), material handling, automation, packaging, printing, solar panels and many other applications which require precise motion control (Fig. 15), the self-powered liquid actuators with the features of high-voltage power source independency, portability and light-weight would make transformative changes to the practical applications. On the other side, as the TENG devices are moving towards a light-weight, high power density and wearable way (Fig. 15), more exciting wearable and flexible TENG powered EWOD devices (*e.g.*, intelligent electronics and health supervision) are foreseeable.

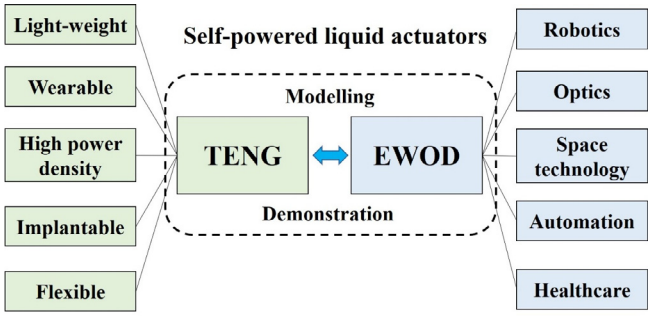

FIGURE 15

Perspectives of TENG powered EWOD devices towards self-powered liquid actuators.

As diverse fancy applications had been demonstrated in the TENG powered EWOD devices, one could find that this field is far from mature in terms of both theoretical modelling as well as experimental demonstration. Extensive and in-depth studies are still needed to address the challenges of:

Please cite this article in press as: J. Tan et al., Materials Today, (2022), https://doi.org/10.1016/j.mattod.2022.07.009

(1) Theoretical modelling: although the phenomenon of using a TENG device for driving aqueous solution on an EWOD device has been widely demonstrated, the theory for modelling the energy conversion process and efficiency is still not established. Theoretical modelling on the TENG powered EWOD liquid actuator helps in-depth understanding the influencing factors to the device. This requires more experimental observation as well as theoretical modelling for correlating the charge transfer process and fluid dynamics.

(2) Understanding the threshold voltage of TENG for EWOD applications: It is known the traditional EWOD devices require a voltage of tens to hundreds of volts to drive. However, the reported TENG powered EWOD device requires a much higher voltage (as compared to commercial power sources) to trigger the EWOD phenomenon. This makes the voltage of TENG difficult to be fitted with the Young-Lippmann equation. Since TENG works as a capacitive power source, the relationship between contact angle modulation with the applied electrostatic energy should be derived in a constant charge mode, instead of constant voltage mode in conventional EWOD devices. More theoretical works for modelling this phenomenon should be investigated in detail.

(3) Miniaturization and automation: Inspired by the requirement in robotics, advanced healthcare and intelligent electronics, the device miniaturization is highly desired. The reported TENG powered EWOD devices are mainly based on a bulky electric motor for TENG conversion. The development of high-voltage, wearable and light-weight TENG triggered liquid actuators towards practical applications requires further study. This can be improved by improving the energy utilization efficiency of TENGs, while further optimizing the materials and structures under the premise of satisfying the application. On the other hand, the electrodes of EWOD devices are complex in some circumstances (*e.g.,* tens to hundreds of electrodes in DMF platform), properly designed control circuit for connecting the TENG and EWOD towards automated devices is desired.

Finally, with the development of material science, system integration, and further exploration of EWOD applications, the TENG driven self-powered liquid actuators will not only broaden the physical understanding of a new type of devices, but also contribute more efforts to diverse practical applications. In the future, with the further clarification of the physical process of TENG-driven EWOD, the miniaturization of equipment and the substantial improvement of device reliability and stability, TENG-powered EWOD devices are expected to be used in self-driven sensing, wearable smart devices, and biomedical fields.

Declaration of Competing Interest

The authors declare that they have no known competing financial interests or personal relationships that could have appeared to influence the work reported in this paper.

Acknowledgements

This work was supported by the National Natural Science Foundation of China (51906031), and the Fundamental Research Funds for Central Universities, DUT20LAB105.

References

[1] G. Lippmann, Ann. Chim. Phys. 5 (1875) 494–549.
[2] H. Dahms, J. Electrochem. Soc. 116 (1969) 1532–1534.
[3] B. Bruno, Comptes Rendus de L'Academie des Sciences Paris Serie II (317) (1993) 157–163.
[4] M.-G. Pollack et al., Lab Chip 2 (2022) 96–101.
[5] R. Sista et al., Lab Chip 8 (2008) 2091–2104.
[6] D. Witters et al., Lab Chip 11 (2011) 2790–2794.
[7] M.-J. Jebrail et al., Lab Chip 12 (2012) 2452–2463.
[8] M. Torabinia et al., Lab Chip 19 (2019) 3054–3064.
[9] R.A. Hayes, B.J. Feenstra, Nature 425 (2003) 383–385.
[10] Y. Chen et al., Nat. Commun. 9 (2018) 1–11.
[11] T. Helps et al., Sci. Robot 7 (2022) eabi8189.
[12] J. Kedzierski, E. Holihan, Sci. Robot. 3 (2018) eaat5643.
[13] K. Choi et al., Annu. Rev. Anal. Chem. 5 (2012) 413–440.
[14] B. Hendriks et al., Opt. Rev. 12 (2005) 255–259.
[15] H. You, A. Steckl, Appl. Phys. Lett. 97 (2010) 023514–023516.
[16] E. Samiei et al., Lab Chip 16 (2016) 2376–2396.
[17] M.-G. Pollack, Electrowetting-based microactuation of droplets for digital microfluidics, Duke University, 2001.
[18] F. Mugele, J.-C. Baret, J. Phys. Condens. Matter 17 (2005) R705–R774.
[19] H. Moon et al., J. Appl. Phys. 92 (2002) 4080–4087.
[20] E. Seyrat, R.-A. Hayes, J. Appl. Phys. 90 (2001) 1383–1386.
[21] M. Dhindsa et al., Thin Solid Films 519 (2011) 3346–3351.
[22] S.-Y. Park et al., Lab Chip 10 (2010) 1655–1661.
[23] D. Jiang, S.-Y. Park, Lab Chip 16 (2016) 1831–1839.
[24] D. Jiang et al., Lab Chip 18 (2018) 532–539.
[25] H. Geng, S.K. Cho, Lab Chip 19 (2019) 2275–2283.
[26] Q. Ruan et al., Sci. Adv. 6 (2020) eabd6454.
[27] M.-H. Shamsi et al., Lab Chip 14 (2014) 547–554.
[28] Y.-H. Chang et al., Biomed. Microdev. 8 (2006) 215–225.
[29] D.S. Millington et al., Digital microfluidics: a future technology in the newborn screening laboratory?, Seminars in Perinatology, Elsevier, 2010.
[30] P.-Y. Keng, R.-M. van Dam, Mol. Imaging 14 (2015) 579–594.
[31] C.-P. Chiu et al., J. Adhes. Sci. Technol. 26 (2012) 1773–1778.
[32] T.B. Jones, Langmuir 18 (2002) 4437–4443.
[33] S.-K. Fan et al., Lab Chip 11 (2011) 343–347.
[34] F.-R. Fan et al., Nano Energy 1 (2012) 328–334.
[35] L. Lin et al., ACS Nano 9 (2015) 922–930.
[36] W. Liu et al., Nat. Commun. 10 (2019) 1–9.
[37] Q. Liang et al., Adv. Mater. 29 (2017) 1604961.
[38] L. Zhou et al., Adv. Energy Mater. 10 (2020) 2002920.
[39] Z.L. Wang, Mater. Today 20 (2017) 74–82.
[40] Z.L. Wang et al., Triboelectric nanogenerator: Vertical contact-separation mode, Triboelectric Nanogenerators, Springer, 2016.
[41] Z.L. Wang et al., Triboelectric nanogenerator: single-electrode mode, Triboelectric Nanogenerators, Springer, 2016.
[42] Z.L. Wang et al., Triboelectric nanogenerator: lateral sliding mode, Triboelectric Nanogenerators, Springer, 2016.
[43] Z.L. Wang et al., Triboelectric nanogenerator: freestanding triboelectric-layer mode, Triboelectric Nanogenerators, Springer, 2016.
[44] D. Jiang et al., Nano Energy 70 (2020) 104459.
[45] X. Xiao et al., Adv. Energy Mater. 9 (2019) 1902460.
[46] Z. Jing et al., Nano Res. 15 (2022) 5098–5104.
[47] Y.-X. Bian et al., Adv. Mater. Technol. 3 (2018) 1700317.
[48] S. Liu et al., Nano Energy 83 (2021) 105851.
[49] Z. Zhao et al., ACS Nano 10 (2016) 1780–1787.
[50] Y. Xu et al., ACS Nano 15 (2021) 16368–16375.
[51] X. Wei et al., ACS Nano 15 (2021) 13200–13208.
[52] D. Zhang et al., Nano Energy 61 (2019) 132–140.
[53] Y. Zi et al., ACS nano 10 (2016) 4797–4805.
[54] S. Cho et al., Nano Energy 71 (2020) 104584.
[55] H. Chen et al., Nano Res. 15 (2022) 2505–2511.
[56] Q. Zheng et al., Adv. Mater. 26 (2014) 5851–5856.
[57] M. Parvez Mahmud et al., Adv. Energy Mater. 8 (2018) 1701210.
[58] M. Xu et al., Nano Energy 57 (2019) 574–580.

Please cite this article in press as: J. Tan et al., Materials Today, (2022), https://doi.org/10.1016/j.mattod.2022.07.009

[59] Y. Wang et al., Nano Energy 78 (2020) 105279.
[60] H. Zhang et al., Nano Energy 2 (2013) 693–701.
[61] S. Zhang et al., Matter 4 (2021) 845–887.
[62] T. Tat et al., Biosens. Bioelectron. 171 (2021) 112714.
[63] Z. Zhou et al., Nat. Electron. 3 (2020) 571–578.
[64] Y. Fang et al., Adv. Mater. 33 (2021) 2104178.
[65] K. Meng et al., Adv. Mater. 34 (2022) 2109357.
[66] X. Liu et al., Adv. Funct. Mater. 32 (2022) 2106411.
[67] J. Sun et al., Adv. Mater. 33 (2021) 2102765.
[66] D.-M. Lee et al., Sci. adv. 8 (2022) eabl8423.
[69] H. Ryu et al., Nat. Commun. 12 (2021) 1–9.
[70] H.-J. Yoon, S.-W. Kim, Joule 4 (2020) 1398–1407.
[71] R. Hinchet et al., Science 365 (2019) 491–494.
[72] X. Chen et al., Small 13 (2017) 1702929.
[73] T. Li et al., Adv. Funct Mater. 26 (2016) 4370–4376.
[74] G. Chen et al., Nat. Electron. 4 (2021) 175–176.
[75] H.-J. Qiu et al., Nano Energy 58 (2019) 536–542.
[76] H. Chu et al., Nano Energy 27 (2016) 298–305.
[77] J. Deng et al., Adv. Mater. 30 (2018) 1705918.
[78] W. Seung et al., ACS Nano 9 (2015) 3501–3509.
[79] H. Guo et al., Sci. Robot. 3 (2018) eaat2516.
[80] M. Shak Sadi, E. Kumpikaite², Nanomaterials 12 (2022) 2039.
[81] G. Chen et al., Chem. Rev. 122 (2022) 3259–3291.
[82] C. Wu et al., Adv. Energy Mater. 9 (2019) 1802906.
[83] Z.L. Wang, Adv. Energy Mater. 10 (2020) 2000137.
[84] F. Yi et al., Adv. Funct. Mater. 29 (2019) 1808849.
[85] G. Zhu et al., Nano Energy 14 (2015) 126–138.
[86] T. Zhao et al., Nano Energy 88 (2021) 106199.
[87] S. Lin et al., Chem. Rev. 122 (2022) 5209–5232.
[88] Q. Ruan et al., Sci. Adv. 6 (2020) eabd6454.
[89] A. Ainla et al., Adv. Mater. 29 (2017) 1702894.
[90] S. Kuiper, B.H.W. Hendriks, Appl. Phys. Lett. 85 (2004) 1128–1130.
[91] J. Li, C.-J.-C. Kim, Lab Chip 20 (2020) 1705–1712.
[92] G. Chen et al., Lab Chip 18 (2018) 1026–1034.
[93] G. Chen et al., Nano Energy 80 (2021) 105524.
[94] D. Jiang et al., ACS Nano 14 (2020) 15394.
[95] H. Li et al., Nano Energy 58 (2019) 447–454.
[96] J. Tan et al., Nano Energy 92 (2022) 106697.
[97] Z.H. Guo et al., Adv. Funct. Mater. 29 (2019) 1808974.
[98] F. Mugele, J.C. Baret, J. Phys.-Condes. Matter. 17 (2005) R705–R774.
[99] Z.L. Wang, Nano Energy 68 (2020) 104272.
[100] Z.L. Wang, Mater. Today 52 (2022) 348–363.
[101] T. Krupenkin, J.A. Taylor, Nat. Commun. 2 (2011) 1–8.
[102] G. Kim et al., Adv. Funct. Mater. 31 (2021) 2105233.
[103] S. Lin et al., Nat. Commun. 11 (2020) 1–8.
[104] Z.L. Wang, A.C. Wang, Mater. Today 30 (2019) 34–51.
[105] J. Zhang et al., ACS Nano 15 (2021) 14830–14837.
[106] F. Zhan et al., ACS Nano 14 (2020) 17565–17573.
[107] X. Li et al., Nat. Phys. 18 (2022) 713–719.
[108] Q. Sun et al., Nat. Mater. 18 (2019) 936–941.
[109] L.E. Helseth, Langmuir 36 (2020) 8002–8008.
[110] H. Zou et al., Nat. Commun. 10 (2019) 1427.
[111] F. Mugele, J. Heikenfeld, Electrowetting: Fundamental Principles and Practical Applications, John Wiley & Sons, 2018.
[112] L. Zheng et al., Adv. Funct. Mater. 27 (2017) 1606408.
[113] J. Nie et al., ACS Nano 12 (2018) 1491–1499.
[114] J. Nie et al., Adv. Mater. Technol. 4 (2019) 1800300.
[115] C.M. Jiang et al., Nano Energy 59 (2019) 268–276.
[116] J. Yu et al., Lab Chip 21 (2021) (2021) 284–295.
[117] J. Wang et al., Nano Energy 66 (2019) 104140.
[118] C. Fang et al., Microsyst. Nanoeng. 6 (2020) 1–9.
[119] C. Wang et al., Nano Energy 98 (2022) 107310.
[120] H. Shen et al., *Adv. Funct. Mater.* (2022) 2204525.
[121] D. Jiang, Energy harvesting and self-powered devices in droplet microfluidics, in: Multidisciplinary Microfluidic and Nanofluidic Lab-on-a-chip, Elsevier, 2022, pp. 361–383.
[122] C.-U. Murade et al., Opt. Express 20 (2012) 18180–18187.
[123] M. Im et al., Langmuir 26 (2010) 12443–12447.
[124] N.-R. Smith et al., J. Display Technol. 5 (2009) 411–413.
[125] J. Lee, Y.H. Won, Opt. Express 30 (2022) 2078–2088.
[126] A. Duduś et al., Appl. Phys. Lett. 105 (2014) 021105.
[127] J. Hsieh et al., IEEE Photon. Technol. Lett. 15 (2003) 81–83.
[128] Z.J. Luo et al., Opt. Rev. 25 (2018) 18–26.
[129] P. Sureshkumar, S.S. Bhattacharyya, J. Adhes. Sci. Technol. 26 (2012) 1947–1969.
[130] Y. Lao et al., J. Display Technol. 4 (2008) 120–122.
[131] W. Zeng et al., Front. Phys. 9 (2021) 642682.
[132] J. Heikenfeld et al., Nat. Photonics 3 (2009) 292–296.
[133] J. Wang et al., MRS Energy Sustain. 6 (2019) 1–23.
[134] Z. Yi et al., Displays 37 (2015) 86–93.
[135] X. Liu et al., Nano Energy 53 (2018) 622–629.
[136] J. Tan et al., Phys. Fluids 33 (2021) 042101.
[137] J. Tan et al., Phys. Fluids (2022), https://doi.org/10.1063/5.0044823.
[138] R. Dey et al., Appl. Phys. Lett. 113 (2018) 243703.
[139] S. Högnadóttir et al., Appl. Phys. Lett. 116 (2020) 073702.
[140] E.D. Wikramanayake, V. Bahadur, Int. J. Heat Mass Tran. 140 (2019) 260–268.
[141] J. Yuan, S.K. Cho, Exp. Fluids 56 (2015) 1–10.
[142] S.H. Byun et al., J. Micromech. Microeng. 25 (2015) 035019.
[143] P. Tian et al., Phys. Fluids 34 (2022) 022104.
[144] X. Li et al., Biomicrofluidics 6 (2012) 011301.
[145] C. Kleinstreuer et al., Int. J. Heat Mass Tran. 51 (2008) 5590–5597.
[146] F. Fontana et al., J. Drug Deliv. Sci. Technol. 34 (2016) 76–87.
[147] C.M.B. Ho et al., Lab Chip 15 (2015) (2015) 3627–3637.
[148] J.-Y. Cheng, L.-C. Hsiung, Biomedical Microdevices 6 (2004) 341–347.
[149] W. Satoh et al., J. Appl. Phys. 103 (2008) 034903.
[150] C.K.W. Koo et al., Analyst 138 (2013) 4998–5004.
[151] C.W. Nelson et al., Lab Chip 11 (2011) 2149–2152.
[152] J. Fukai et al., Phys. fluids 7 (1995) 236–247.
[153] F.J. Hong et al., J. Micromech. Microeng. 22 (2012) 085024.
[154] Y. Mita et al., Solid-State Electronics 53 (2009) 798–802.

Please cite this article in press as: J. Tan et al., Materials Today, (2022), https://doi.org/10.1016/j.mattod.2022.07.009